A critical discussion on the analysis of buried interfaces in Li solid-state batteries. Ex situ and in situ / operando studies.

Isidoro López, Julien Morey, Jean-Bernard Ledeuil, Lénaïc Madec, Hervé Martinez

Journal of Materials Chemistry A

A critical discussion on the analysis of buried interfaces in Li solid-state batteries. *Ex situ* and *in situ*/*operando* studies.

Journal:	*Journal of Materials Chemistry A*
Manuscript ID	TA-PER-05-2021-004532.R1
Article Type:	Perspective
Date Submitted by the Author:	14-Sep-2021
Complete List of Authors:	López, Isidoro; IPREM, Morey, Julien; IPREM Ledeuil, Jean-Bernard; University of Pau /CNRS, IPREM/ECP Madec, Lénaïc; IPREM, ; Martinez, Herve; Universite de Pau et des Pays de l'Adour, IPREM CNRS UMR 5254

ARTICLE

A critical discussion on the analysis of buried interfaces in Li solid-state batteries. *Ex situ* and *in situ*/*operando* studies.

Received 00th January 20xx,
Accepted 00th January 20xx

DOI: 10.1039/x0xx00000x

Isidoro López,[a*] Julien Morey,[a] Jean Bernard Ledeuil,[a] Lénaïc Madec,[a,b*] and Hervé Martinez[a,b*]

Interfacial electro-chemo-mechanical phenomena determine the performance of Li solid-state batteries (SSBs), thus the study of these processes is key to construct more efficient and stable systems. In this regard, the analysis of interphases, including their evolution during cycling, is probably the most challenging aspect in the field of SSBs, as interfaces in these cells are inherently buried. In this perspective, a critical discussion on the various methodologies currently employed to gain access to buried interfaces and obtain reliable structural and chemical information is provided. Since this aspect is commonly overlooked in the literature, a particular focus has been addressed to rigorous procedures allowing to achieve reproducible and unambiguous results. Simultaneously, the valuable structural, electronic and chemical data collected on interphases by using these robust methods is presented. It is also shown that the development of strategies to probe buried interfaces has paved the way to progress in attractive *in situ* and *operando* measurements. On the other hand, new experiments carried out in our laboratory evidence that ion etching for depth profiling analysis, which is widely used to study solid electrolyte interphases (SEIs) and cathode electrolyte interphases (CEIs) in liquid and solid-state Li batteries, is not convenient to elucidate the distribution of chemical components in composite materials present in SSBs due to sensitivity of certain compounds like Li salts to ion bombardment. Finally, our discussion can be extended to other important materials and nanostructures presenting buried interfaces such as layered films with applications in photovoltaics and core-shell nanoparticles.

1. Introduction.

Lithium solid-state batteries (SSBs) are currently recognized as the most promising technology for the next generation of Li rechargeable batteries.[1–5] In these systems, the liquid electrolyte of common Li ion batteries (LIBs) is replaced by a solid electrolyte, which plays the dual role of Li ion conductor and separator between the electrodes. Thus, the electrochemical properties of SSBs, such as capacity fading and rate capability, are mainly governed by two key aspects: 1) the ionic and electronic conductivity of the solid electrolyte, and 2) the chemical and structural characteristics and stabilities of the diverse solid/solid interfaces into the system. A significant progress has been achieved in the synthesis of solid electrolytes exhibiting ionic conductivities comparable to the one from liquid electrolytes (10^{-3} – 10^{-2} S cm^{-1}) and there are numerous reviews addressing the main advantages and drawbacks of oxides, sulfides, polymers and composites working as solid electrolytes (see for instance refs. [3,6–12]).

The existence, formation and evolution of interphases in SSBs leads to energetic barriers for Li ion diffusion and electron transfer, thus the improvement of their electrochemical performance can only be achieved through a comprehensive understanding of the electro-chemo-mechanical properties of materials at solid/solid interfaces before and during cycling.

Recently, a few reviews have addressed the study of interphases in SSBs from a merely descriptive point of view[13–17] by discussing the main chemical/structural information obtained from diverse analytical techniques. However, a critical discussion on suitable methodologies to gain access to the inherently buried interfaces in SSBs (see below) and reliably probe their morphological, structural and chemical properties has never been considered until now. Indeed, a survey of the literature on SSBs shows plenty of examples on spectroscopic and microscopic characterization of solid/solid interfaces, but almost no report mention how these buried interfaces could be analysed (see for instance refs. [18–22]) and a few of them describe procedures that depend on the manual skills of a researcher to separate mechanically two connected phases (see for instance refs [23–26]). Obviously, these approaches are questionable for sound reasons. Firstly, the probed material could not correspond to the interphase as, commonly, there is no justification or discussion about the region selected for analysis. This situation is worst when the sample preparation procedure is not described in the experimental section because the reader cannot even intend to replicate the measurement, which constitute the basis of the scientific knowledge.[27] A second controversial issue concerns the preservation of the structural and chemical integrity of the inner interphase when two materials are mechanically separated. It seems of common

[a] Universite de Pau et des Pays de l'Adour, E2S UPPA, CNRS, IPREM, 64000 Pau, France.
[b] Réseau sur le Stockage Electrochimique de l'Energie (RS2E), FR CNRS 3459, Hub de l'Energie, 80000 Amiens, France.

sense that the mechanical effort exerted to carry out the separation will lead to partial or total destruction of the morphology of the interphase. Chemical degradation effects resulting from this operation have never been assessed in the literature, but they cannot be discarded in the absence of a systematic study. The last source of controversy relates to the homogeneity and thickness of the interphase. When two adjacent materials are mechanically separated, the original interphase is split in two films, each on covering one of the separated materials. The surface of the two coatings can be then probed; however, the spatial interpretation of the results is challenging as the exact depth position of the analysed region in the full thickness of the original interphase is unknown and the chemical composition of the interphase has been showed to be not homogeneous. In this context, the most widespread approach[24,28–30] to tackle this problem consists in performing depth profiling studies in which sequential steps of material sputtering *via* ionic bombardment and spectroscopy/spectrometric analysis are combined to reconstruct the chemical composition of the interphase through its thickness (see section 5 for more details). In this perspective, we provide experimental results warning about this strategy. Particularly, when SSBs containing polymer or composite solid electrolytes are studied. Another more exotic approach to gain insight on the depth profile composition of the interphase relies on manually etching increasing amounts of the film with a scalpel.[31] This operation was reported to allow for controlling the removing of 5 μm of material. However, the full validity of this approach remains to be proved by replication of the experiments and application of the same methodology to distinct SSBs.

The lack of rigorous analysis in most of current contributions dealing with interfacial phenomena in SSBs had led us to write this perspective. We aim at providing a critical discussion of contributions exploiting robust and rigorous methodologies to obtain reliable and valuable information of interphases in SSBs. These methodologies can be categorised into two approaches. The first one relies on the combination of a suitable sample preparation procedure or the use of modified conventional batteries with the subsequent application of an analytical technique, usually a surface analytical technique, to gather structural and/or chemical data. In this perspective, this strategy is called *The Uncovering approach*. The alternative rigorous approach consists in the direct use of analytical techniques featuring large sampling depth (SD) on SSBs. SD refers to the thickness of the surface of material that can be probed by a particular technique. For certain methods, SDs can achieve values as large as probe a significant volume or the full battery. In this perspective, this strategy is called *The Bulk approach*.

The advantages and limitations of the methodologies used in the two approaches will be critically evaluated. Furthermore, we will discuss relevant examples illustrating the interest in the application of the two approaches to unravel electro-chemo-mechanical phenomena in SSBs.

Additionally, we will see that the proper application of robust methodologies to probe buried interfaces in SSBs paves the way to the implementation of *in situ*/*operando* measurements, where the chemical and structural analysis of the interphase during electrochemical cycling is carried out without the necessity of battery dissembling or handling. This kind of experiments avoid sample pollution and deleterious processes associated to relaxation of the battery, both of them found in *ex situ* analysis[32–35] where the SSB must be previously dissembled and mounted on a sample holder.

Finally, our perspective must not be regarded as a statement of invalidation of previous results obtained from the less rigorous approaches described above. A number of these works have provided fundamental insight on electro-chemo-mechanical phenomena in SSBs. A supplementary objective of our discussion is stimulating the acquisition of new data with the presented more reliable methodologies for allowing comparison with this previously obtained information.

2. The challenge: buried interfaces.

A significant number of interfaces can be found in SSBs. Considering an electrochemical cell where Li metal is employed as negative electrode (anode), the electro-chemo-mechanical properties of materials in the following interfaces need to be evaluated (**Figure 1**):

A) *Negative electrode:* grain boundaries, Li/bulk solid electrolyte, Li/impurity.

B) *Bulk solid electrolyte:* grain boundaries, materials interfaces in composite electrolytes (e.g. polymer/inorganic filler).

C) *Positive electrode:* grain boundaries, composite electrode/bulk solid electrolyte, active material/solid electrolyte, active material/conductive additive, solid electrolyte/conductive additive, current collector/active material, current collector/conductive additive and current collector/solid electrolyte.

There are some aspects and simplifications in the list and in **Figure 1** which deserve comments.

1. The composite electrode/bulk solid electrolyte interface is complex and contains actually diverse kinds of interfaces, but, for analysis purposes, some experimental measurements validate their simplification as a formally single interface in most cases.[36,37]
2. When a composite negative electrode is used (e.g. graphite or Si/C blends), the same interfaces listed above for the positive electrode must be considered.
3. Grain boundaries, namely, interfaces between two grains of the same material exhibiting distinct crystallographic orientations, are not depicted in **Figure 1** for the sake of simplicity. However, it is important to note that these interfaces play a key role in the performance of the battery as it will discussed in the manuscript.

4. In addition to the existence of interfaces between different materials, SSB are characterized by the presence of a significant amount of voids. In LIBs, these spaces are commonly filled by the liquid electrolyte providing an ionic pathway for Li diffusion. In SSBs, the presence of voids cannot be completely suppressed even after pressing the cathode/solid electrolyte/anode stack.

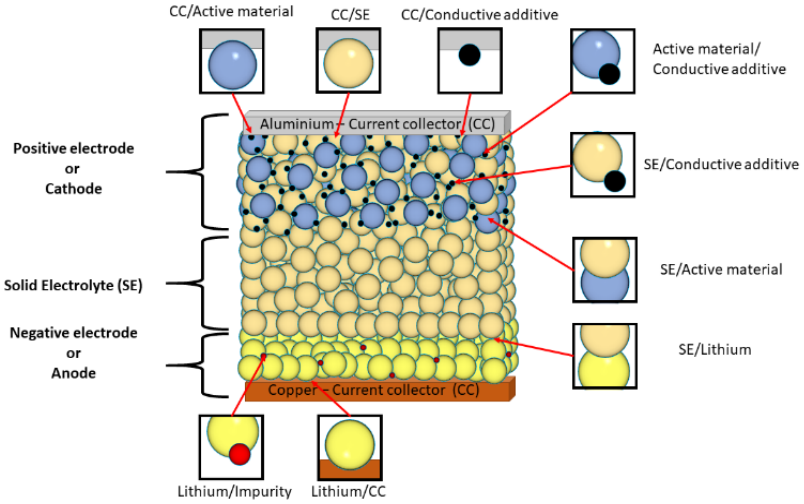

Figure 1. Schematic illustration of buried interfaces existing in Li-metal SSBs.

Since the formation and evolution of voids are usually associated to interfacial phenomena, we will include them in our discussion in spite of they are not explicitly indicated or mentioned in the list and in **Figure 1**.

The rigorous analysis of all the interfaces in SSBs is not trivial, as they are buried in the sense that two adjacent materials cannot be easily separated to probe the nature and structure of the interphase. Furthermore, separation of the two materials can lead to a deterioration of the chemical and structural characteristics of the interphase and a loss of relevant information.

It is surprising that a significant amount of work in the literature on the analysis of interfaces in SSBs does not describe the procedure undertaken to gain access to them and/or the adopted precautions to ensure that the analysed region is representative of the whole studied interphase (see for instance refs.[38,39]). Additionally, an important number of publications base their spectroscopic surface analysis on the manual ability of the researcher to separate mechanically the interfaces (see for instance refs. [26,31]).

In the interest of the increasing research activity on materials chemistry of interphases in SSBs, we provide a rich overview of rigorous experimental methodologies that can provide, in our own opinion, reliable and valuable information on their electro-chemo-mechanical properties. However, this does not mean that all previous conclusions drawn from less rigorous approaches are wrong. As it was stated above, previous less reliable experiments have shed light on interfacial processes in SSBs.

The first part of this perspective is devoted to a critical discussion of the two main rigorous approaches explored until now in the field of SBBs to study structural and chemo-electro-mechanical phenomena in these energy storage devices. Firstly, the *Uncovering approach* will be considered (section 3). In this strategy, the objective is the study of one or several interphases by a particular analytical technique, usually a surface analytical technique. These originally buried interphases must be previously exposed by using a convenient sample preparation procedure. We will describe the fundamentals, advantages and drawbacks of each procedure, and provide relevant examples of application in SSBs. Similarly, we will discuss the different surface analytical techniques that can be employed in this approach and the remarkable results gathered. Secondly, the *Bulk approach* will be scrutinised (section 4). This approach tries to circumvent the necessity of sample preparation procedures by the direct application of analytical techniques featuring large SDs to the study of the battery. Again, the principles, advantages and drawbacks of each method will be evaluated. Several outstanding examples illustrating the interest of this strategy will be also presented. Importantly, it will be evidenced that these two rigorous approached have paved the way to the development of *in situ*/*operando* measurements allowing to obtain reliable results on interfacial processes in SSBs.

The last part of this perspective addresses the suitability of performing depth profiling experiments based on ion milling for the chemical analysis of interphases in SSBs (section 5). Since this practice is very common in the field and is usually carried out after the mechanical or manual separation of materials, an evaluation seems convenient to avoid misinterpretation of results.

3. The Uncovering approach: Methodologies based on exposing buried interfaces.

The most obvious strategy to gain access and probe buried interfaces in SSBs consists in a two steps procedure: 1) exposing the surface of the diverse materials contained in the electrochemical cell, and 2) Analyse the treated sample by a surface technique. Therefore, this section is divided into two sub-sections addressing each step

3.1.Methodologies to expose buried interfaces.

The simplest procedure relies on the separation of two adjacent materials and the subsequent analysis of the two surfaces which were originally in contact. Despite this methodology has been extensively used, the separation of connected phases can be extremely challenging or impossible. Furthermore, it introduces

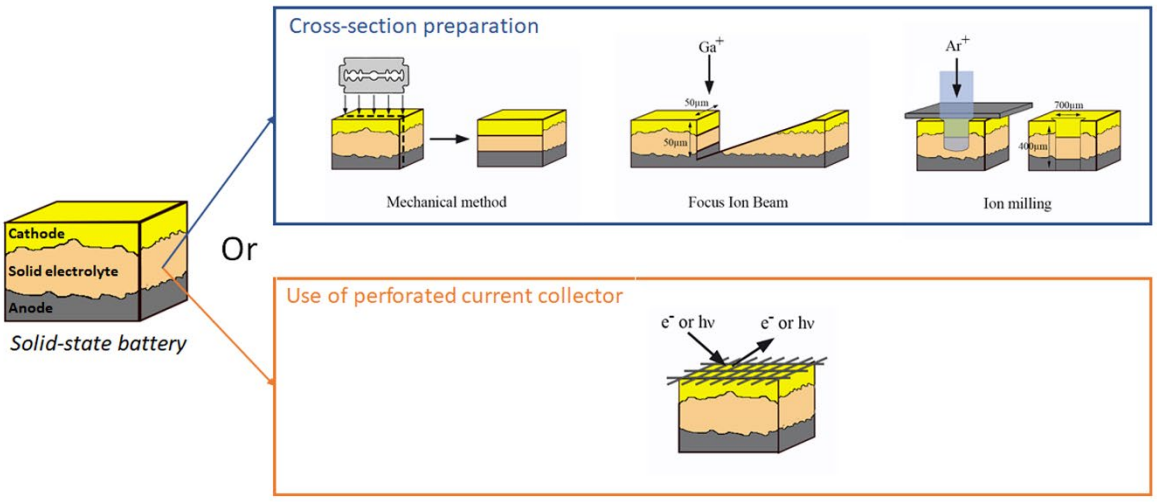

Figure 2. Current rigorous methodologies used to expose interfaces in SSBs allowing their subsequent reliable analysis.

a source of controversy, as the detachment of the bulk solid electrolyte from Li and composite electrodes is most often carried out manually. Thus, the exact location of the interphase as well as its morphology and chemical composition depend on the manual ability of the researcher and the spatial region chosen for the subsequent analysis. Considering the lack of reliability in this approach, experimental results obtained following this methodology will not be discussed in the perspective.

In contrast, two more robust and reproducible strategies allowing for revealing buried interfaces are (i) the preparation of cross-sections and (ii) the utilization of perforated current collectors. In the next sections, a critical discussion of these two sample preparation methods used to reveal buried interfaces in SSBs is provided (**Figure 2**).

3.1.1. Preparation of cross-sections.

In this approach, a clear cross-section of the SSBs containing well-defined and stacked cathode/solid electrolyte/anode layers is exposed by the action of a particular technique. Thus, the interfaces can be easily visualized by electronic and/or optical microscopy, and subsequently analysed by a wide range of both bulk and surface analytical techniques. The preparation of cross-sections offers a more powerful and rigorous alternative to probe buried interfaces since it is less dependent on the manual skills of the researcher and; thus, it can provide more reliable and reproducible results. Additionally, cross-sections potentially enable the evaluation of all the interfaces listed in section 2, while the strategy of separation of adjacent phases only gives access to Li/bulk solid electrolyte and composite electrode/bulk solid electrolyte interfaces.

Despite the numerous advantages, the analytical approach based on the preparation of cross-sections is not exempt from some challenges and drawbacks. The first issue is a practical aspect. Two of the possible methodologies to prepare cross-sections, mechanical methods and broad ion beam (BIB) polishing, are carried out in an equipment separated from the instrument where the cross-section will be probed. Therefore, the sample containing the cross-section must be correctly mounted in a sample holder suitable for the analysis and transferred to the analytical instrument under air-free conditions, usually by means of a transfer vessel. Placing properly the cross-section on the sample holder is not trivial as the cross-section should lie perfectly flat regarding to the sample holder. This is particularly important for experiments in scanning probe microscopy (SPM) as inclination angles of the cross-section will lead to erroneous interpretations of the results. The situation is ever more challenging when the cross-section must be analysed by more than one technique because sample holders from different instruments are not usually compatible. In order to address this challenge, Atsushi Sakuda *et al.* have successfully developed a single sample holder allowing for performing BIB polishing and the analysis of the prepared cross-section by SPM and scanning electron microscopy - energy-dispersive X-ray spectroscopy (SEM-EDS) in the three different instruments.[40]

Another adventitious problem with cross-sections prepared by mechanical methods or BIB polishing is pollution due to sample handling for changing of sample holder or contact with the atmosphere of the gloves box. This fortuitous degradation can makes difficult, in some cases, probing the chemical composition of cross-sections with surface analytical techniques, particularly with methods characterised by thin sampling depths like time-of-flight secondary ion mass Spectrometry (ToF-SIMS).

The last challenges of cross-section are common to the three methodologies (mechanical methods, focused ion beam (FIB) and BIB polishing) and it is exclusively associated to *in situ/operando* experiments. As it will detailed in section 3.2, *in situ/operando* measurements involve the preparation of the cross-section previously to the application of an electrochemical method (e. g. galvanostatic cycling). Since the

cross-section to be analysed after or during the electrochemical input lies at one edge of the battery, it can exhibit a different reactivity as compared to the material buried in the bulk of the battery. In other words, the cross-section could suffer from edge effects. Evidences of such a phenomenon have been provided by *in situ* ToF-SIMS experiments.[41] Finally, external pressure applied to *in situ*/*operando* cells based on cross-sections is significantly lower and less homogeneous than the one holding more conventional SSBs. As a consequence, electro-chemo-mechanical phenomena observed at interfaces in this kind of experiments can differ from the actual processes leading to the degradation of performance in more conventional SSBs, particularly for batteries containing fully inorganic solid electrolytes. Importantly, non-homogeneous pressure also exacerbates asymmetric deformation of Li by creeping of this soft metal on the side of the battery occupied by the cross-section. This effect, often overlooked in the literature,[42] has been thoroughly studied by SEM.[43]

In the next sub-sections; we will present in detail the three different methodologies that have been proposed for the preparation of cross-sections in SSBs so far. The fundamentals and the particular advantages and drawbacks of each procedure will be discussed.

3.1.1.1. Mechanical methods.

Two procedures have been used to mechanically obtain cross-sections of stacked materials in SSBs. The simplest one relies on the employment of manual cutting tools like common or ultrasonic knifes and blades.[20,44–47] However, this experimental approach is not very convenient to preserve the morphology of the layered structure in SSBs, as the solid electrolyte is commonly made of very brittle materials like metal oxides or very ductile compounds like polymers.

An alternative mechanical technique, which is particularly suitable for electrolytes based on polymers, is cryo-microtomy.[48] This method consists in the controlled sectioning of a material with a glass or diamond knife at extremely low temperatures (-185 °C).[49] The procedure can be carried out in commercially available instrumentation and lead to a freestanding thin section (0.5 – 5 μm) of the material and a new and flat surface created in the sample block where the thin section was cut out. The two pieces of material can be then probed by diverse spectroscopic, microscopic and spectrometric techniques. At cryogenic temperatures, ductile materials like polymers become brittle, as the temperature is lower than the glass transition temperature, T_g, and the sectioned samples preserve their internal structure. Therefore, interfaces in composite and layered materials are clearly distinguished. Although the method is slightly laborious, it provides well defined cross-sections which better preserve the morphology of the original materials in SSB stacks.

The only example in the literature of the application of cryo-microtomy to a SSB has been reported by researchers at the Canadian company Hydro-Québec.[48] They obtained a cross-section (**Figure 3A**) where four well-defined layers of the $LiNi_{0.6}Mn_{0.2}Co_{0.2}O_2$ (NMC 622)/PEO:LiTFSI(30:1)/Li battery are discernible (the fourth layer corresponds to the Al current collector in the cathode). Despite this attractive result, cryo-microtomy was unable to reveal clearly the microstructure of the composite cathode (**Figure 3C**). In contrast, it will be shown that FIB (section 3.1.1.2) and BIB polishing (section 3.1.1.3) are more powerful sample preparation procedures to preserve and delineate the microstructure of composite electrodes (grains, grain boundaries, voids and amorphous material).

3.1.1.2. Focused ion beam (FIB).

In the context of SSBs, this sample preparation technique consists in milling the stack of materials with a small ion beam (15 - 50 nm), usually Ga^+, to create a cross-section where the layered structure is clearly revealed. In order to provide a wide cross-section (50 – 100 μm) the ion beam must be scanned ("rasterized"). Another attractive application of FIB consists in the extraction of an extremely thin lamellae of the layered material from a solid-state microbattery. This thin section can be subsequently analysed by (Scanning)Transmission Electron Microscopy (S)TEM in combination with other associated and powerful spectroscopic methods (see below) like electron energy loss spectroscopy (EELS) and selected area electron diffraction (SAED). A detailed and visual description of this sample preparation methodology in the field of SSBs has been recently published.[50]

The preparation of cross-section by FIB presents a significant advantage regarding to mechanical methods and BIB polishing. The FIB procedure is commonly carried out in the same instrument, under high vacuum conditions, where the analytical measurement will be performed. Thus, there is not necessity for transfer of the prepared cross-section and the sample remains

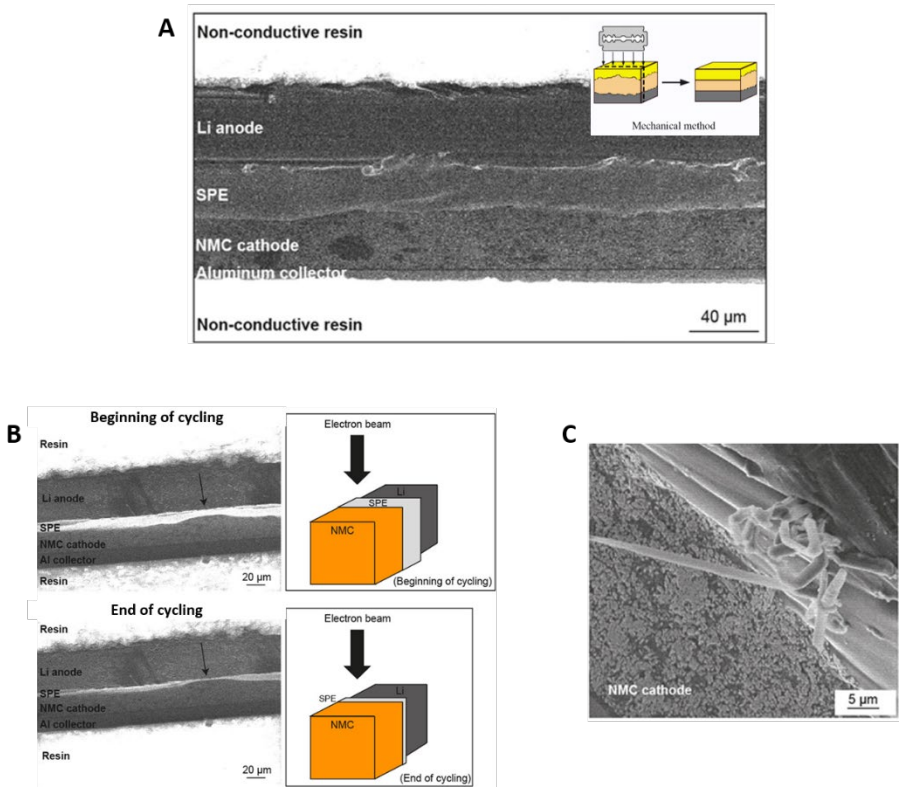

Figure 3. (A) Image recorded by SEM of a cross-section from a NMC 622/PEO:LiTFSI(30:1)/Li battery prepared via cryo-microtomy. (B) Images recorded of the same cross-section at the beginning and the end of a galvanostatic cycling experiment monitored *in situ* by SEM. A dramatic thinning of the polymer solid electrolyte is clearly observed at the end of cycling. (C) Image recorded by SEM of the same cross-section showing the formation of Li dendrites after galvanostatic cycling. Note the poor resolution of the microstructure of the NMC cathode achieved by cryo-microtomy. Figures adapted with permissions from reference 48. Copyright (2020) American Chemical Society.

always under high vacuum conditions limiting adventitious chemical deterioration of the exposed surface.

Excellent examples of the usefulness of FIB to expose buried interfaces inside composite cathodes have been recently published by the group of Jürgen Janek.[51–53] In these studies, cross-sections of cathodes containing NMC 622, thiophosphate-based solid electrolytes and, in some cases, a carbonaceous conductive additive (super C65 or vapor-grown carbon fibers, VGCF) were prepared by FIB directly inside the analysis chamber of a ToF-SIMS instrument. The microstructure of the composite electrode is clearly discernible in the image of the cross-section recorded by secondary electrons (SE) detection (**Figure 4A**). This well-defined microstructure contrasts with the poorly resolved one obtained after cryo-microtomy (**Figure 3C**).

Despite the potential of FIB to prepare clear cross-sections, a recent work by Y. Shirley Meng *et al.* warns about the extensive employment of this technique at room temperature to study SSBs, particularly with Li metal anodes.[54] The interaction of the Ga^+ ions with the diverse surfaces can lead to a local increase of temperature triggering a chemical and structural deterioration of the materials. In the case of Li anodes, this effect results in a severe morphological degradation. As a more reliable alternative, cryo-FIB preserves the structural characteristic of Li and it should be privileged to prepare cross-sections containing temperature-sensitive materials like polymers and associated composites.

A potential drawback of FIB is the small dimensions of the obtained cross-sections. Typical values are 50 µm width x 50 µm depth for a milling time of approximately 3.5 h with a 30 kV Ga^+ gun. Although these values are indicative as they depend on the sputtering rate of each material. Bigger dimensions could always be achieved at the expanse of increasing the milling time; however, this approach would lead to unpractical sample preparation times and accumulative damage of the exposed cross-section. The small area and particular geometry of cross-sections elaborated by FIB thus rise two concerns: 1) the exposed region could be no representative of the chemical composition and structure of the whole material; and 2) the geometrical disposition of the sidewalls of the crater eroded by

ARTICLE

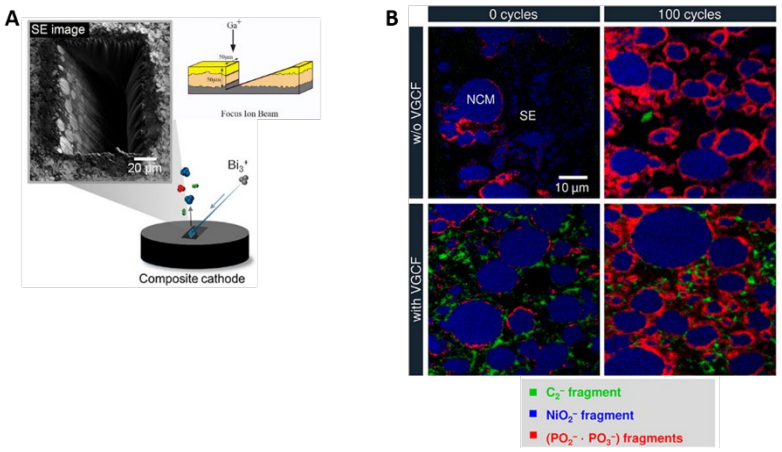

Figure 4. (A) Image recorded by SE detection of a cross-section from the cathode of a NMC 622/β-Li_3PS_4 /Li battery prepared by FIB inside the analysis chamber of a ToF-SIMS instrument. Note the good resolution of the microstructure of the composite electrode. (B) Images recorded by ToF-SIMS of four different FIB-prepared cross-sections of two composite cathodes, differing in the presence or absence of the conductive additive VGCF, before and after galvanostatic cycling. Selected fragments were exploited to construct the images. Thus, C_2^- is representative from VGCFs, NiO_2^- from NMC 622 and PO_2^- and PO_3^- from interphases containing phosphate or phosphite. Figure adapted with permissions from reference 52. Copyright (2020) American Chemical Society.

FIB is not suitable for the source-detector angle configuration of certain spectroscopic setups like in conventional XPS instruments.

The emergence of a new FIB gun based on Xe plasma can resolve the limitation associated to the small dimensions of cross-sections created by the ionic Ga^+ beam. Cross-sections exposed by this new device are significantly bigger as a consequence of an increased sputtering rate. Indeed, it has been reported that materials removal by Xe plasma FIB is 60 times faster than in conventional Ga^+ FIB.[55] Furthermore, the Xe plasma FIB leads to less surface damage in the exposed cross-section.[56] To the best of our knowledge, this technique has never been applied as sample preparation method to study buried interfaces in SSBs; however, it has been successfully used to acquire large 3D images of composite electrodes by successive steps of Xe plasma FIB and SEM analysis (see below).[57,58] Areas with dimensions in the order of 500 µm could be sputtered within dozens of minutes. This dimension value is similar to the one achieved by Broad Ion Beam (BIB) polishing (see below).

3.1.1.3. Broad Ion Beam (BIB) polishing

BIB polishing is a sample preparation procedure which consists in etching one edge of the sample with a parallel and broad beam of energetic ions, usually Ar^+.[59] To be effective in the preparation of cross-sections, the sample must be covered by a masking plate which lets unprotected only the small volume of material that will be etched. The principle of the technique is the same as in FIB, in the sense that a cross-section with well-defined interfaces is obtained as a result of the sputtering of a surface layer of the stacked material with high-energy ions. However, the broader ion beam makes the surface area sputtered by BIB polishing significantly larger for similar operation times[59] (around 700 µm width x 400 µm depth *vs* 50 x 50 µm for typical FIB) and it is a cheaper and less time-consuming method. The energy of the Ar^+ beam can be varied

ARTICLE

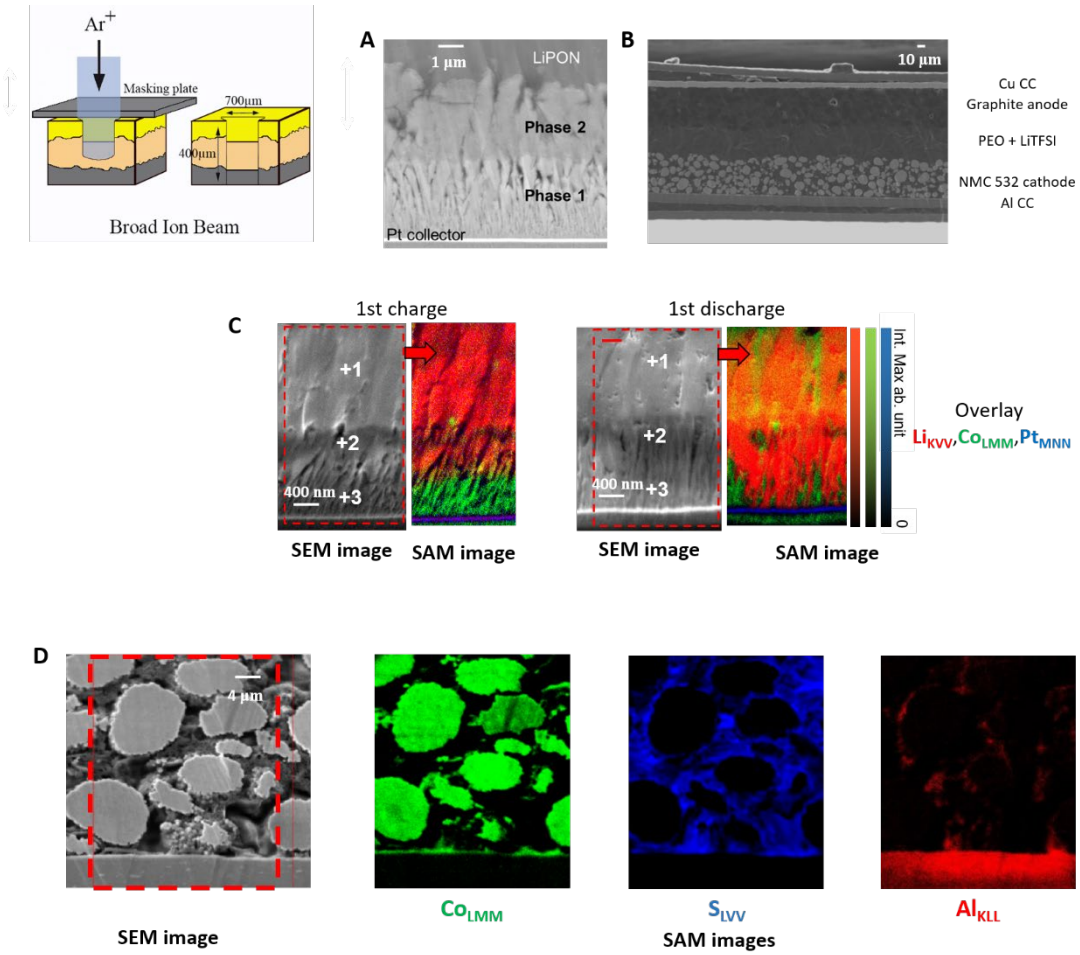

Figure 5. (A) Image recorded by SEM of a cross-section from a LiCO/LiPON/Li microbattery prepared by BIB polishing at RT. (B) Image recorded by SEM of a cross-section from a NMC 532/PEO:LiTFSI/Graphite battery prepared by BIB polishing at 133 K. Note the excellent resolution of the microstructure of the cathode compared to cryo-microtomy and the large dimensions of the cross-section compared to FIB. (C) Images recorded by SEM and SAM of two different cross-sections from the microbattery in (A) after fist charge and discharge. (D) Images recorded by SEM and SAM of the cross-section in (B) focused on a region near the Al CC/cathode interface. Note the coherent distribution extracted from SAM for NMC (Co_{LMN} signal), polymer-LiTFSI blend infiltrated in the cathode (S_{LVV} signal) and CC (Al_{KLL} signal). Figures (A) and (C) adapted with permissions from reference 63. Copyright (2017) American Chemical Society.

to optimize the rate of polishing or prevent decomposition of the remaining non-sputtered material. The technique is highly convenient to expose the diverse materials contained in heterostructured samples like mesoporous and stacked materials[60,61] or core-shell nanoparticles.[62]

Despite the potential of BIB polishing to uncover buried interfaces, there are only a few reports exploiting this sample preparation method for the subsequent analysis of SSBs.[36,41,63,64] Thus, for instance, this procedure allowed us to characterize unambiguously interphases in solid-state microbatteries (section 3.2.6.1) by scanning electron microscopy (SEM), auger electron spectroscopy (AES) and scanning auger microscopy (SAM).[63] The SEM image of the cathode/solid electrolyte interface in the cross-section of a $LiCoO_2$ (LCO)/LiPON/Li microbattery prepared by BIB polishing reveals unambiguously the presence of three distinct phases (**Figure 5A**). One phase corresponds to the LiPON solid electrolyte and the other two (phase1 and phase2) are ascribed to the LCO active material as it will be detailed in section 3.2.6.1. An adventitious side effect of BIB polishing is damage of a thin layer of material surface because, as in FIB, the ion beam leads to local heating triggering the degradation of the morphology and chemical state of temperature-sensitive materials like lithium and polymers. This aspect is particularly relevant in the

ARTICLE

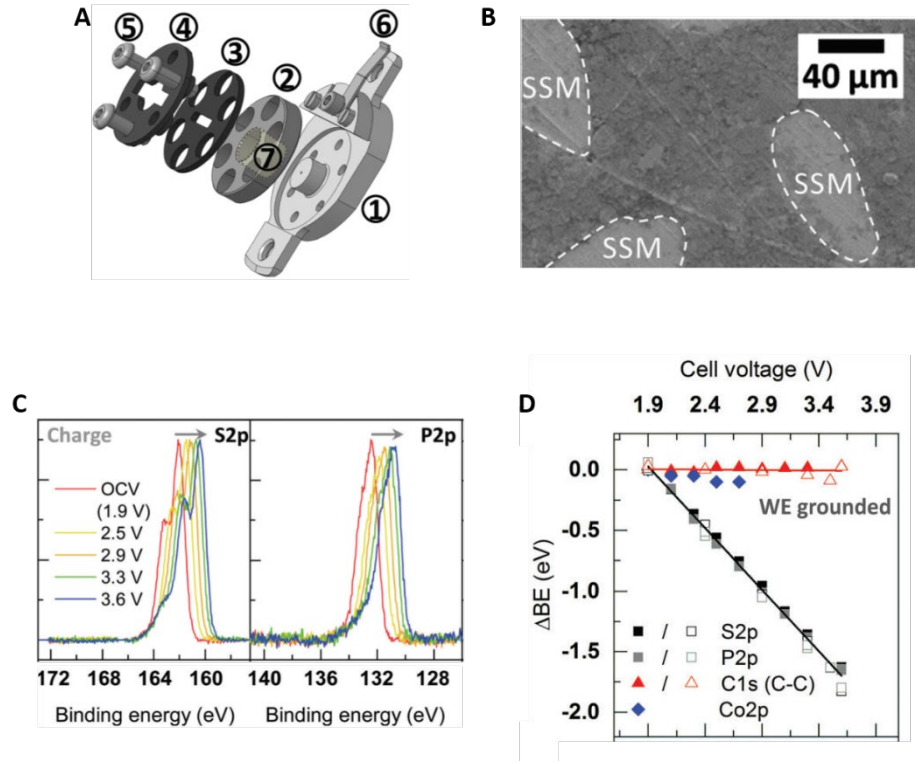

Figure 6. (A) Schematic drawing of the spectroelectrochemical cell developed by the group of Mario El kazzi for *operando* XPS experiments on SSBs. (B)Top-view image recorded by SEM of a $LiCoO_2/(Li_2S)_3–P_2S_5$(LPS)/$InLi_x$ battery showing the surface of the composite cathode including the network of the stainless steel mesh (SSM) which plays the role of perforated current collector. (C) *Operando* monitoring of shifting in the core level S 2p and P 2p spectra of peaks associated to the solid electrolyte during charge of the aforementioned battery. In this experiment, the cathode was grounded. (B) Plot of shifting in BE for diverse peaks associated to materials in the cathode during charge when the cathode is grounded. Since the solid electrolyte is an electric isolator, its associated peaks shift at lower BEs with increasing electrochemical potentials. Since LCO and carbon electronic additive are electric conductors, their associated peaks do not shift because they follow the polarisation of the battery. Figures adapted from Ref. 66 with permission from the PCCP Owner Societies.

perspective of applications in the field of SSBs, in which lithium, organic (macro)molecules and other temperature-sensitive materials are usually present. Fortunately, technical progress has allowed carrying out BIB polishing under cryogenic conditions.[65]

Indeed, we present in this perspective preliminary experimental results from our group illustrating the interest of cryo-BIB polishing to prepare cross-sections of a classical SSB: $LiNi_{0.5}Mn_{0.3}Co_{0.2}O_2$ (NMC 532)/PEO:LiTFSI/Graphite. The image obtained by SEM of the cross-section shows all the layers of the three main components of the battery, including the Al and Cu current collectors (**Figure 5B**). The interfaces are easily recognizable and the microstructure of the composite cathode is fully revealed. A comparison between this image and the cross-section prepared by cryo-microtomy (**Figure 3C**) highlights the better performance of BIB polishing to probe in-depth the microstructure of large sections of composite electrodes. Thus, the distribution of active material, polymer containing Li salt and Al current collector could be unambiguously stablished by scanning auger microscopy, SAM (**Figure 5D**). Importantly, although similar analysis can be undertaken with methodologies exploiting FIB as sample preparation procedure, a comparison between the images in **Figure 4A** and **Figure 5B** illustrate the larger dimensions, and thus representability of results, of cross-sections prepared by BIB polishing.

On the other hand, a common challenge in the analysis of cross-section prepared by BIB polishing is changing of sample holder after ion etching as BIB polishing and analytical measurement are carried out at different instruments. As discussed in the introduction of section 3.1.1, this operation can ruin the analysis step. A significant advancement to overcome this issue

has been recently developed[40] by Atsushi Sakuda *et al.*, which was also discussed in the introduction of section 3.1.1.

3.1.2. Use of perforated current collectors.

The simplest approach to analysis interfaces in a composite cathode (containing active material, conductive additive and binder) without the necessity of disassembling or mechanical cutting would be probing the battery through the face covered by the Al current collector (top of the battery in **Figure 1**). However, this strategy is not usually feasible. Common current collectors present thickness between 10 – 15 μm. All the analytical surface techniques discussed in section 3.2 displays SD in the order of some tens of nanometers, except EDX and RAMAN in which it increases to 1 – 6 μm. Therefore, probing the battery through the face covered by the current collector would result in signal produced exclusively from this material precluding the study of the buried interfaces. The easiest solution to overcome this physical problem is assembling the SSB with a current collector exhibiting holes.

Holes in the current collector allows passage of radiation or electron beams which can directly interact with the uncovered surface of the electrode. Obviously, the radiation or electron ejection resulting from this interaction can also traverse the holes to be detected. As a consequence, some of the buried interfaces near the current collector side of the battery are exposed and can be probed. The thickness of the probed region depends on the SD of the used microscopic/spectroscopic technique. This approach is highly convenient for the development of several *in situ* and *operando* methods in the field of SSBs. Relevant examples of *operando* XPS studies on SSBs based on perforated current collectors have been reported by the group of Mario El Kazzi.[66–68] In these experiments, a special cell design allowed for using a stainless steel mesh as perforated current collector (**Figure 6A**,**B**).

Despite this approach is highly attractive, it has four drawbacks. Firstly, only interphases near the current collector can be probed as a result of the limited SD of common and synchrotron-based spectroscopic techniques (SDs in the range of 10 – 30 nm *vs* electrodes with a thickness in the range of 40 – 100 μm). Thus, only information form this region, which is not representative of the whole electrode, can be collected. The second inconvenience relies on the possible inhomogeneity of electronic conduction pathways within the composite electrode as a consequence of porous structure of the current collector.[34] Thirdly, similarly to *in situ*/*operando* experiments performed on cross-sections, pressure in SSBs with perforated current collectors is not as efficient as the one holding batteries with conventional current collectors. Indeed, Mario El Kazzi *et al.* have reported recently a slight degradation of the electrochemical performance of their cell for *operando* XPS measurement regarding to a conventional cell without perforated current collector.[68] This effect was tentatively attributed to the less efficient pressure holding the *operando* cell and it should be more critical for SSBs made of fully inorganic solid electrolyte, where the applied pressure seems to have a stronger influence to decrease porosity and favour intimate contact between solid electrolyte and active material.[69] Finally, residual analytical signal from the current collector material can partially overlap signals from materials inside the composite cathode disturbing the interpretation of some results. For instance, the Fe 3p peak in the XPS spectrum of a stainless steel mesh, like the one employed by Mario El Kazzi and coworkers, has similar binding energy to the Li 1s peak.[66]

3.2. Analysis of exposed buried interfaces.

Once the buried interfaces have been uncovered by means of a reproducible and reliable methodology, they can be analysed by a particular technique or a combination of them. At this point of our discussion, it is important to realize that much of the interest of the analysis of interphases in SSBs is placed on elucidating their chemical and structural evolution as a result of the application of an electrochemical input. In other words, the aim of the analysis is usually unveiling chemo-electro-mechanical phenomena at interfaces triggered by battery charge and discharge. Therefore, we define three distinct possibilities of analysis in the context of the present perspective:

Ex situ analysis: the analysis is carried out on a sample prepared from a battery which has been subjected to an electrochemical input and subsequently disassembled.

In situ analysis: the battery, which has been previously modified or treated with one of the aforementioned sample preparation procedures, is introduced inside the analysis chamber or special cell of the instrument. The electrochemical input can then be applied to the battery in this place, but the analysis of the interphase is only carried out after interruption of the electrochemical input. Switching between electrochemical input and analytical measurement allows for monitoring the evolution of the interphase.

Operando analysis: it is similar to the *in situ* analysis; however, probing of the interphase is performed simultaneously to the application of the electrochemical input. This operation mode enables to follow in real time the evolution of the interphase.

The next sections will present a critical discussion about the diverse methods and most relevant associated results that have been applied to the *ex situ* and *in situ*/*operando* study of exposed buried interfaces in SSBs (**Figure 7**) In view of the similarity between *in situ* and *operando* experiments, we have preferred to combine in a single section for the sake of simplicity.

3.2.1. Studies based on optical microscopy (OM).

OM has been mainly adapted to perform operando measurements on SSBs.[45,70,71,71–75] A notable example of this approach is the study of lithiation of a graphite electrode in a graphite/LPS/$InLi_x$ battery reported by Akitoshi Hayashi's group.[45] Optical mapping of a cross-section of the cell showed a gradual decrease of the degree of lithiation in the whole electrode after 4 cycles; however, the loss of capacity in Li insertion was more severe at the current collector/solid electrolyte interface. The cross-sections was prepared by mechanical cutting with a tungsten blade.

In another interesting study,[72] the cross-section of a S_8/PEO:LiTFSI(20:1)-LLZTO/Li SSB prepared by cutting with a ceramic knife was analysed by *operando* OM. Importantly, the measurements proved the irreversible dissolution of polysulfides into the solid electrolyte during the first discharge at temperatures in which the ionic conductivity of the electrolyte and the electrode/electrolyte charge transfer resistance are more favourable. Polysulfides dissolution and subsequent shuttling to the anode is a well-known capacity-fading process in liquid Li-S batteries.[76] Solid electrolytes have been proposed as a solution to this problem because they can act as physical barriers.[77] However, this work illustrates the incapacity of "solid electrolytes" with low melting temperatures to avoid polysulfide shuttling during cycling at moderate-high temperatures (55 °C – 75 °C).

3.2.2. Studies based on scanning electron microscopy (SEM) and energy-dispersive X-ray spectroscopy (EDS).

3.2.2.1. *Ex situ* studies.

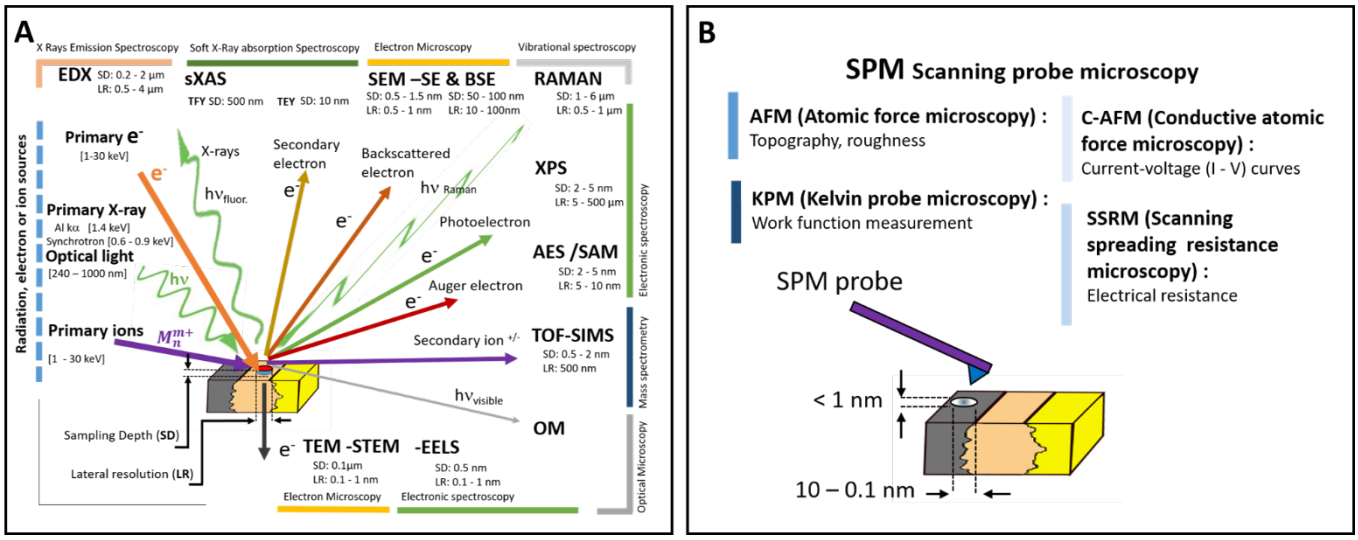

Figure 7. Overview of main analytical techniques currently used for the study of exposed buried interfaces in SSBs based on the interaction of radiation, electrons or ions (A) and atomic probes (B) with the uncovered surfaces of the diverse materials. The figure represents experiments carried out on well-defined prepared cross-sections; however, a number of the techniques depicted in A have also been applied to surfaces exposed following the strategy of perforated current collector (see text for more details). Sampling depth (SD) refers to the thickness of the surface of material than can be probed with a particular techniques and Lateral resolution (LR) refers to the ability of a particular technique for distinguish two distinct points on the surface of the material.

SEM, alone or in combination with EDS, is the most popular technique for the *ex situ* analysis of cross-sections in SSBs. There are numerous examples in the literature on the utilization of this electron microscopy to visualise cross-sections prepared by FIB,[78–80] BIB polishing[63,69] or mechanical cut.[47] Since a comprehensive compilation of all these reports is out of the scope of this perspective and the amount of information collected from this method is rather limited, we will focus on the potential of FIB-SEM tomography as a valuable and less-explored tool to gain access to the mechanical evolution of the morphology of composite electrodes at different stages of their cyclelife. In FIB-SEM tomography, sequential steps of FIB and 2D SEM imaging are repeated to reconstruct a 3D image of a small region of the electrode.[81] Gerbrand Ceder *et al.* have recently exploited this approach[82] to assess the evolution with cycling of the microstructure of the composite cathode in a $LiNi_{0.5}Mn_{0.3}Co_{0.2}O_2$ (NMC 532)/$75Li_2S$–$25P_2S_5$ (LPS)/$InLi_x$ battery. The volume occupied by active material, solid electrolyte, conductive additive and voids was identified and calculated from back-scattered electrons (BSE). The experiments evidenced a large increase of the volume of voids from 2.87 vol% (pristine) to 9.50 vol% after 50 cycles leading to a loss of surface contact between active material and other solid state components of the cathode. This phenomenon could explain the observed capacity fading. Indeed, mechanical degradation of electrodes due to the loss of solid-solid interfaces or particle cracking is recognized as a critical challenge in the development of efficient and long cycle life SSBs.[83–85] Therefore, FIB-SEM represents a highly attractive method to evaluate the evolution of the microstructure of the diverse components in SSBs with a spatial resolution less than 100 nm.[82,86] However, the volumes of material probed by this technique are relatively small (60 µm × 40 µm × 30 µm for the experiments carried out by Ceder and coworkers), thus, the analysed region could be no representative of the mechanical behaviour of the whole material. Alternatively, the study of the microstructure of larger volumes can be carried out with X-ray computed tomography, X-CT (section 4.2), although resolutions comparable to FIB-SEM are only attainable with synchrotron X-ray sources.[87]

3.2.2.2. *In situ/operando* studies.

Laboratories at the Canadian company Hydro-Québec have extensively exploited the mechanical preparation of cross-sections to carry out *in situ* SEM analysis of diverse cycling SSBs containing PEO:LiTFSI solid electrolyte.[48,88–91] Although most of the reports do not mention the procedure followed to expose

cross-sections, the last contribution specifies the use of cryo-microtomy, as it was discussed in section 3.1.1.1.[48]

The most attractive application of *in situ* SEM is the possibility of visualising in real-time the variation in thicknesses of the three stacked materials (composite cathode, solid electrolyte and Li anode) and consequently the position of the associated interfaces. For instance, a gradual thinning of the polymer solid electrolyte due to compositional degradation occurred during galvanostatic cycling of a NMC 622/PEO:LiTFSI(30:1)/Li cell.[48] This phenomenon is marked with an arrow in **Figure 3B**. The growth of dendrites from the Li/solid electrolyte interface was also observed. Importantly, EDS analysis on these dendrites shows the presence of C, O and Li suggesting that these structures are made of lithium carbide which could originate from polymer reduction.

3.2.3. Studies based on transmission electron microscopy (TEM) or scanning transmission electron microscopy (STEM) and associated techniques.

3.2.3.1. *Ex situ* studies.

The preparation of thin cross-sections suitable for robust and reproducible TEM/STEM studies is usually carried out by applying FIB to previously fabricated micro SSBs (*vide supra*).[50,92,93] It is a highly complex process which requires a sound expertise. One prominent example of this approach was reported by Y. S. Meng and coworkers.[94] They created a $LiCoO_2$/LIPON/Si nanobattery by the operation of FIB on the corresponding microbattery. Subsequently, the nanobattery was electrochemically charged at different states inside the FIB instrument. A final thinning step by FIB of the nanobattery at different states of charge allowed to perform *ex situ* scanning TEM in combination with electron energy lose spectroscopy (EELS). The measurements on the overcharged state unravel the existence of three phenomena: the evolution of a detrimental Li accumulation region at the $LiCoO_2$/LIPON interface, the clear formation of a new phase at the LIPON/Si interface containing Li, P and Si, and the deposition of metallic Li at the Si/Cu (current collector) interface. The development of all these new interphases could explain the capacity fading of the nano-electrochemical cell.

3.2.3.2. *In situ*/*operando* studies.

In situ and *operando* studies based on TEM and STEM are gaining an increasing interest to assess interfacial processes in SSBs.[13,95,96] The utility of this approach is not limited to the analysis of the chemical composition and structure of interphases by the combination of TEM/STEM and EELS, SAED, or annular bright-field micro (ABF) and high-angle annular dark-field (HAAF) detection.[33,97–101] The extension and magnitude of the electric double layer or space-charge layer (SCL) at electrode/solid electrolyte interfaces can also be evaluated.[102,103] The SCL arises from the build-up of opposite charges at the electrode/electrolyte interface. It is present in the uncycled SSBs due to differences in chemical and electric potentials between the two solids, eventually triggering the formation of interphases;[104,105] and it is obviously enhanced by the variation of electrochemical potential of the electrode during battery cycling. A paramount example of the relevance of *in situ*/*operando* TEM/STEM-based techniques to probe the SCL is the pioneering study of the cathode/solid electrolyte interface in a $LiCoO_2/Li_{1-x-y}Al_yTi_{2-y}Si_xP_{3-x}O_{12}$/Pt solid-state microbattery carried out by K. Yamamoto and coworkers.[102] A combination of FIB thinning, TEM and electron holography (EH), a technique capable of measuring the distribution of the electric potential through a section of the microbattery, revealed the formation of a SCL at the analysed interface of approximately 1.5 µm thickness. This value is much higher than the theoretical Debye length expected for a double-charged layer (in the range of a few Å). However, a more recent *ex situ* study,[106] mainly based on the combination of TEM with EH and spatially resolved EELS, on an uncycled $Cu/Li_{1+x+y}Al_x(Ti,Ge)_{2-x}Si_yP_{3-y}O_{12}$ (LASGTP)/Cu solid state system shows the formation of a significantly thinner SCL (around 10 nm) at the Cu/LASGTP interface. Although these findings suggest that more research efforts should be devoted to clarify the thickness and magnitude of the SCL, it has been proposed that this double layer has a small impact in the charge transfer resistance at the electrode/electrolyte interface.[104,107]

Despite *in situ* measurements based on TEM and associated techniques have showed great promise to unravel fundamental electro-chemo-mechanical phenomena at the buried interfaces in SSBs, this experimental approach presents some limitations. Firstly, it can be only implemented on small electrochemical cells like micro and nano-batteries. These devices consist in a stack of well-defined micrometric layers of cathode, solid electrolyte and anode with the eventual formation of interphases and are of high interest in the framework of powering small electronic devices. However, SSBs for applications in e-mobility and grid storage contain composite cathodes (eventually also composite anodes and solid electrolytes) characterized by the presence of numerous interfaces. Therefore, the chemical and physical events responsible for the electrochemical performance can diverge between the two systems. Additionally, the thickness of cross-sections elaborated by FIB for *in situ* TEM-based measurements is of a few tens of nanometers. At these dimensions, electro-chemo-mechanical phenomena and the reactivity of the materials could be radically different, including an enhanced deterioration by electron beam damage.[108] Finally, the problem of reduced and non-homogeneous stack pressure for *in situ*/*operando* cells cross-sections discussed in section 3.1.1 is particular relevant in measurements relying on (S)TEM and associated techniques. In these cells, the only stack pressure is exerted by the tip of a micromanipulator.

3.2.4. Studies based on Auger electron spectroscopy (AES) and scanning Auger microscopy (SAM).

3.2.4.1. *Ex situ* studies.

As introduced in the ToF-SIMS section (3.2.4.2), the analysis and visualization of spatial distribution of Li compounds with spectroscopic methods based on the excitation by X-rays beams is challenging due to the small cross-section associated to the Li

element. AES and SAM offer an attractive solution to this issue as Li produces relatively good signals. Additionally, SAM can provide a lateral spatial resolution in the range of 5-100 nanometers.[109] Despite these advantages, AES and SAM present a challenge which is shared with all the techniques using electron irradiation as source: degradation of electronically non-conductive materials due to thermal degradation triggered by surface charging.[110] This deleterious effect is particularly critical for polymers and organic molecules. Indeed, several solutions have been proposed to mitigate problems associated to surface charging and heating. For instance the use of additional electron or positive ion beams for charge compensation[111] and measurements on thin sections of polymer under cryogenic conditions.[112]

A remarkable and rigorous example of the application of AES and SAM for the analysis of interphases in SSBs was recently published by our group.[63] In order to obtain reliable and reproducible results, cross-sections of a LiCO/LiPON/Li microbattery were prepared by BIB polishing, as discussed in section 3.1.1.3, and the exposed cathode/solid electrolyte interface was probed by AES and SAM. The formation of a Li-rich interphase was clearly evidenced in the uncycled battery, which is in agreement with previous FIB-STEM/EELS studies.[97] Furthermore, the detection of Li allowed for interrogating on its reversible desertion/insertion in the two phases contained in the cathode after the first charge/discharge (**Figure 5C**).

3.2.4.2. *In situ*/*operando* studies.

To the best of our knowledge, there is only one example of a truly *in situ* SAM and AES experiment on SSBs.[43] A $LiNi_{0.80}Co_{0.15}Mn_{0.05}O_2/Li_6PS_5Cl/Li$ battery was analysed, but, unfortunately, the cross-section of the device were prepared by manual cutting. The formation of dendrites was clearly observed during electrochemical cycling. The surface composition of these structures was consistent with the presence of oxidized Li (e.g. Li_2O); however, the formation of this species on the surface of dendrites can be explained by the reaction of metallic Li with residual water still present at ultra-high vacuum conditions.

3.2.5. Studies based on RAMAN spectroscopy and microscopy.

3.2.5.1. *Ex situ* studies.

As for XPS and ToF-SIMS experiments, RAMAN measurements on SSBs are relatively popular but they are commonly performed on samples without a reliable and robust preparation procedure. An outstanding exception is the mapping study of the composite positive electrode/solid electrolyte interface in a $LiCoO_2$/LPS/$InLi_x$ battery published by Masahiro Tatsumisago and co-workers.[37] A cross-section of the sample was prepared by BIB polishing and the exposed flat interface was probed by RAMAN microscopy. The preferential formation of detrimental Co_2O_3 at the interface, far from the current collector, was evidenced after the first charging process.

3.2.5.2. *In situ*/*operando* studies.

The most relevant work was recently reported by Laurence J. Hardwick and co-workers.[113] They exploit the strategy of perforated current collectors to probe buried interfaces in a $LiCoO_2/Li_6PS_5Cl/Li$ battery. An optically transparent window was partially coated with a thin (50 nm) Au film which played the role of current collector. A central round area of the window was not covered by the metal and it allows the pass of a laser beam to carry out *operando* RAMAN spectroelectrochemistry. The analysis of interfaces inside the composite $LiCoO_2$ electrode and the Li_6PS_5Cl/Li interface revealed the formation of ionic isolating Li_2S, S and P_2S_x containing interphases, in agreement with previous results obtained by diverse *ex situ* spectroscopic techniques.[16]

3.2.6. Studies based on X-ray photoelectron spectroscopy (XPS).

3.2.6.1. *Ex situ* studies.

XPS is the most widely used method to study the chemical evolution of interfaces in SSBs. Paradoxically; almost all the reported experiments rely on the analysis of the surface of the materials obtained after the manual separation[23,24,26,114–117]or manual etching[31,47] of the electrode/solid electrolyte interface. These operations can be easier for the Li/solid electrolyte interface, but in all cases, the procedures lack reproducibility and raise concerns about if interphases are being actually probed. The scenario is still worst in a remarkable number of papers in which the sample preparation method is not even mentioned.[20,21,25,38,39,118] Therefore, we encourage reviewers to discuss critically the robustness and reliability of the methodologies employed to gain access to the buried interfaces analysed by XPS measurements.

Instead of these questionable sample preparation methods, two more reliable approaches have already been used for *ex situ* XPS studies. The first one consists in the utilization of synchrotron radiation to carry out variable-energy hard XPS and it will be discussed in the section devoted to the *Bulk approach* as this technique exhibits a relatively large SD which can be exploited to probe buried interfaces in microbatteries without the necessity of sample preparation procedures or the modification of the device. The second strategy consists in the deposition of a very thin layer of Li metal on the solid electrolyte inside the XPS analysis chamber[119] or in a connected preparation chamber.[120] The procedure is ideal to assess the intrinsic chemical reactivity of the electrolyte with a Li electrode, but it is restricted to the study of this interface. Furthermore, it has been recently showed that the reactivity of a $Li_{6.25}Al_{0.25}La_3Zr_2O_{12}$ solid electrolyte varies depending on Li is deposited by electron beam evaporation or magnetron sputtering.[121]

3.2.6.2. *In situ*/*operando* studies.

The group of Mario El Kazzi has reported[66–68] probably the most outstanding examples of how perforated current collectors can be exploited to perform *operando* monitoring of the electrochemical evolution of interfaces in SSBs. In their first pioneering contribution,[66] they analysed the cathode of a $LiCoO_2/(Li_2S)_3–P_2S_5$(LPS)/$InLi_x$ system employing a stainless steel

mesh as perforated current collector. This experiment not only revealed the chemical composition of degradation products at solid electrolyte/active material and solid electrolyte/conductive additive interfaces, but also differences in surface potential between the varied components into the positive electrode, including interphases, offering a complete picture of potential profile inside the composite cathode (**Figure 6C,D**).

As it was already discussed in section 3.1.2, the last experiments carried out by El Kazzi and co-workers suggest a decrease in the electrochemical performance for *operando* cells with perforated current collectors.[68]

3.2.7. Studies based on time-of-flight secondary ion mass Spectrometry (ToF-SIMS).

3.2.7.1. *Ex situ* studies.

A survey of the literature data on the utilization of ToF-SIMS for the analysis of buried interfaces in SSBs reveals the same issue found in XPS measurements: the sample preparation procedure. Most of the publication are based on the analysis of surfaces manually separated or cut.[122] Notable exceptions to this common practice have been recently reported[51–53] by Jürgen Janek *et al.* for NMC 622/Li_6PS_5Cl/InLix, NMC 622/LPS/Li and NMC 622/Li_6PS_5Cl/$Li_4Ti_5O_{12}$ batteries. Cross-sections of the composite cathodes were prepared by FIB in the ToF-SIMS instrument, as previously discussed in section 3.1.1.2, and the exposed surfaces were subsequently analysed. In one of their contributions,[52] images from composite cathodes containing or lacking VGCF as conductive additive were constructed from characteristic negative ion fragments from NMC 622, VGCF and phosphate degradation products (**Figure 4B**). The measurements showed unambiguously an increase of the amount of phosphates at the active material/solid electrode interface after electrochemical cycling in both composite electrodes.

3.2.7.2. *In situ* studies.

The first *in situ* study on a SSB has been published by Nobuyuki Ishida and co-workers.[41] They assembled a symmetric $LiCoPO_4$/Co-$Li_{1-x}Al_xGe_{2-x}(PO_4)_3$/$LiCoPO_4$ cell in which the composite cathode material contained a mixture of $LiCoPO_4$ as active material, Co-$Li_{1-x}Al_xTi_{2-x}(PO_4)_3$ as solid electrolyte and Pd particles as conductive additive. In order to expose the interfaces, the battery was subjected to BIB polishing. The subsequent elemental distribution mapping of the cross-section by ToF-SIMS evidenced partial reversible delithiation/lithiation of the active material that decreases with increasing cycling. An irreversible delithiation of the solid electrolyte was also observed after the first discharge pointing out the formation of a space charge layer. Interestingly, this study identifies one possible limitation of *in situ*/*operando* experiments carried out with cross-sections: exposed surfaces can exhibit a reactivity and electro-chemo-mechanical behaviour radically different to the material beneath. Indeed, ToF-SIMS experiments showed that any change in Li composition could not be detected during electrochemical cycling unless a thin layer (roughly 20 nm) of material was sputtered from the exposed surface previously to the measurement.

Recently, Yamagishi *et al.* have reported operando measurements on a $LiNi_{0.8}Co_{0.15}Al_{0.05}O_2$/LPS/$InLi_x$ SSB.[123] A cross-section of the battery was prepared by FIB and the evolution of the chemical composition of the materials, including their spatial distribution, inside the composite cathode was probed by operando ToF-SIMS. The experiments showed the interest of ToF-SIMS as a powerful technique to track the diffusion of Li atoms, which is extremely challenging with most of the methods. Thus, this technique allows for interrogating the degree of reversible (de)lithiation of active material particles. Furthermore, PO_x^-, SO_x^- and S_2^- fragments associated to the oxidation of LPS could be detected. Importantly, the intensity of SO_3^- fragment exhibits a variation compatible with previously observed[124] redox activity of the associated interphase, namely, it increases during charging and decreases after discharging.

3.2.8. Studies based on soft X-ray absorption spectroscopy (sXAS).

3.2.8.1. *Ex situ* studies.

In sXAS, highly bright synchrotron radiation is exploited as X-ray source to illuminate the sample at varied wavelengths. In the context of SSBs, most studies rely on the detection in reflection mode of the photoelectrons, total electron yield (TEY) detection, or X-ray fluorescence, total fluorescence yield (TFY) detection, generated as a consequence of the radiation-sample interaction. In these experiments, the absorption spectra of the sample in energy regions associated to low energy transitions of transition metals are commonly recorded, e.g. 840 – 890 eV for Ni L-edge, thus, the penetration depth of the technique is relatively low and it can be considered as a surface analytical tool. Notwithstanding, higher energy synchrotron radiation can also be used as bulk methods, e.g. in computed X-ray nanotomography or hard X-ray absorption spectroscopy (hXAS). A brief discussion of the application of these techniques in SSB will be provided in section 4.

In SSBs,[34] sXAS is a common method to track the evolution of the oxidation state of transition metals in the cathode and, thus, it gives no information about the chemical composition of interphases. However, the combination of TEY and TFY detection in sXAS experiments can provide valuable information on metal oxidation states at interfaces involving active materials. The penetration depth of these two detection techniques is significantly different. Indeed, the thickness of the probed region in TEY detection is around 10 nm, while it is around 500 nm in TFY detection.[125] Therefore, the combination of the two detection modes can reveal a gradient in metals oxidation states on the surface of the particles, including interfaces.

For instance, this strategy has been recently exploited[23] by Xueliang Sun *et al.* to show the beneficial effect of a protective lithium niobium oxide coating on a $LiNi_{0.8}Mn_{0.1}Co_{0.1}O_2$ (NMC 811) cathode. The SSB contained PEO:$LiClO_4$/$Li_{6.4}La_3Zr_{1.4}Ta_{0.6}O_{12}$ (LLZTO) as solid electrolyte and Li as anode. The combination of

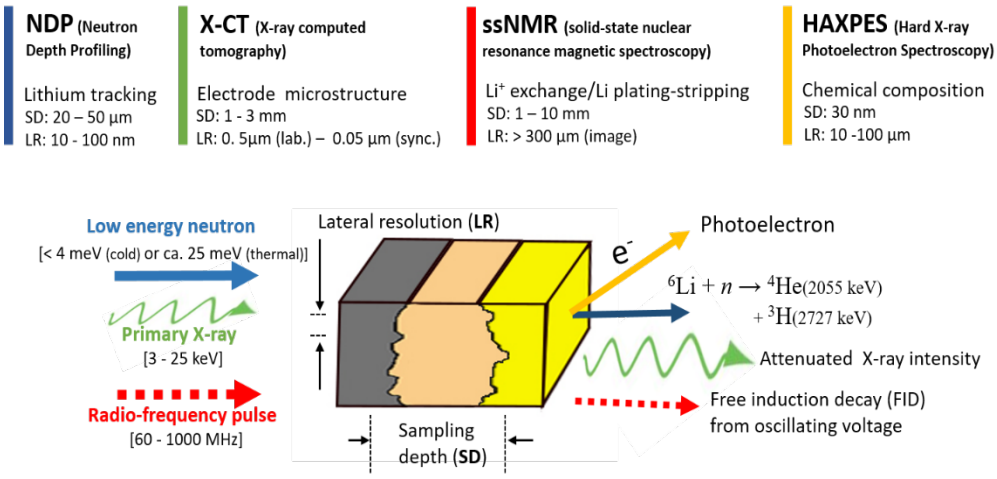

Figure 8. Overview of main analytical techniques used in the bulk approach to probe buried interfaces in SSBs.

TEY/TFY detection suggested that the surface of the coated active material suffers a slight structural degradation while the bulk remains intact after 5 galvanostatic cycles. In contrast, the unprotected material suffers a more severe degradation at both the surface and the bulk. Unfortunately, the samples of the analysed NMC 811 electrodes were obtained after mechanical cutting of the cycled batteries and there is no indication of which precautions were adopted to assure the reproducibility and representability of the XAS spectra.

3.2.8.2. *In situ/operando* studies.

Perforated current collectors have been successfully used in *in situ* and *operando* sXAS studies of cathodes in SSBs. In a pioneering work,[34] Wanli Yang *et al.* elaborated an Al current collector containing ordered holes with 50 µm diameter. The modified Al foil was then used as current collector for either composite NMC 111 or $LiFePO_4$ (LFP) cathodes. In the two SSBs, PEO:LiTFSI (10:1) was used as solid electrolyte and Li as anode. In the NMC 111 system, the spectroscopic evolution of the oxidation state of Ni was consistent with the electrochemically derived state of (dis)charge of the battery. In contrast, in the LFP cell, the spectroscopically measured oxidation state of Fe evidenced a heterogeneous distribution of the metal oxidation state inside the composite electrode. Indeed, active material near the current collector seems to be more electrochemically active than the same material near the solid electrolyte separator. Interestingly, homogeneous redistribution of Fe oxidation state was reached after a relaxation period (4 – 40 hours) at open circuit voltage. The authors explained the different behaviours for NMC 111 and LFP cathodes as the result of their distinct charge conductivities, (de)lithiation mechanisms and microstructures.

Adopting the strategy of perforated current collectors, Carlos A. F. Vaz *et al.* have recently showed[126] the possibility to study the chemical composition of interphases by *in situ* and *operando* sXAS. The experiments evidenced the formation of Li_2CO_3 and Li_2O in the graphitic areas of a composite graphite electrode after Li insertion in a graphite/LiI doped LPS/$InLi_x$ battery.

3.2.9. Studies based on scanning probe microscopy (SPM).

3.2.9.1. *Ex situ* studies.

Besides topographic studies carried out by atomic force microscopy (AFM), SPM techniques have been barely implemented for *ex situ* analysis of interfaces in SSBs. An interesting example of the application of advanced SPM methods to assess interfacial phenomena has been reported by Kaiyang Zeng and co-workers.[127] Electrochemical strain microscopy (ESM) was used to evaluate the diffusion of Li^+ at the nanoscale level inside a $Li_{1+x}Al_xGe_{2-x}(PO_4)_3$ (LAGP) solid electrolyte with glass-ceramic structure. As sample preparation method, the roughness of the LAGP pellet was smoothed by polishing with sandpaper and subsequent short thermal etching to remove the damaged surface of the material. The ESM experiments evidenced the emergence of strain at grain boundaries due to Li^+ accumulation after local negative polarization of the surface.

More recently, Atsushi Sakuda *et al.* have published an outstanding study[40] combining three different SPM techniques and SEM/EDS measurements to assess the electrical properties of a composite cathode, containing only the active material and the solid electrolyte, in a $LiNi_{0.33}Mn_{0.33}Co_{0.33}O_2$ (NMC 111)/LPS/Li battery. In order to prepare a flat and reproducible cross-section of the layered sample, BIB polishing was carried out under cryogenic conditions (-100 °C). Importantly, the prepared cross-section could be transferred between BIB polishing, SPM and SEM/EDS instruments under air-protected conditions in the same sample holder without requiring dismounting. As discussed in section 3.1.1, this new design of sample holder represents a significant advance as it is known that exposed cross-sections are extremely sensitive to manipulation, mainly due to two reasons. First, the clean newly created surface can be rapidly polluted as a consequence of manual operations to change the sample from sample holder. Second, the cross-section should lie perfectly flat regarding to the sample holder. This is particularly important for SPM experiments as inclination angles of the cross-section will lead

to erroneous interpretations of the results. In their study, Atsushi Sakuda *et al.* used SEM/EDS to find unambiguously the spatial distribution of active material and solid electrolyte aggregates and particles inside the cathode. Regarding to SPM techniques, Kelvin probe microscopy (KPM) was exploited to unravel differences in work function of the two materials; scanning spreading resistance microscopy (SSRM) provided differences in electrical resistances; and conductive atomic force microscopy (C-AFM) was employed to record punctual I-V curves on diverse particles or agglomerates. This multi-technique approach led to two main observations. First, overall, the electrical resistance of active material particles decreases after charging except for particles with single-point contact with other NMC 111 particles. Second, there is a slight gradient of work function values (qualitatively comparable to redox potential) for NMC 111 particles through the thickness of the composite electrode after charging the battery. Active material particles near the solid electrolyte separator exhibit a lower work function than particles near the current collector. These results suggest the occurrence of low electronic pathways inside the composite electrode which is detrimental for its performance; however, it is worth to mention that the composite electrodes did not contain carbonaceous electronic conductive additives.

3.2.9.2. *In situ/operando* studies.

As stated above, SPM methods can be powerful and unique tools to track *in situ* or *operando* the potential drops created in SSBs after electrochemical polarisation. In two separated contributions,[36,64] Hideki Masuda *et al.* showed that *in situ* and *operando* Kelvin probe microscopy (KPM) can be exploited to unravel differences in work function of materials inside the composite cathode and at the composite cathode/solid electrolyte interface in a $LiCoPO_4$/Co-$Li_{1-x}Al_xTi_{2-x}(PO_4)_3$/Co-$Li_{1-x}Al_xGe_{2-x}(PO_4)_3$/Co-$Li_{1-x}Al_xTi_{2-x}(PO_4)_3$/Pd anode free SSB. Importantly, the sample was prepared by BIB polishing. The experiments demonstrated the formation of a sharp potential drop region at the composite cathode/solid electrolyte interface with a rough thickness of 1 µm, suggesting the creation of a space charge layer. Again, this value is significantly larger than the expected one from the Gouy-Chapman model and it is in agreement with the result of a previous *in situ* TEM-EH study,[102] but significantly larger than the value calculated from *ex situ* TEM-EH&EELS.[106]

4. The Bulk approach: Methodologies based on techniques featuring large sampling depths.

Conventional microscopy (optical and electron), spectroscopic and spectrometric techniques for materials analysis exhibit a low sampling depth. As a consequence, only the firsts 10 – 100 nm of the surface are actually probed with these methods. This constraint explains why exposing buried solid/solid interfaces is the most indicated and reliable procedure to study them. Our previous discussion has illustrated the strength of this approach as well as associated limitations.

However, it exits some analytical techniques, suitable for the study of buried interfaces in SSBs, which present a larger penetration depth allowing the investigation of some of the materials in the cell without the need of dissembling, cutting or ion milling procedures. Among these methods (**Figure 8**), the most common are neutron depth profiling (NDP), micro- and nano-X-ray computed tomography (X-CT) and nuclear magnetic resonance (NMR). Electrochemical impedance spectroscopy (EIS) is another attractive and widespread bulk method allowing for monitoring the formation and evolution of interphases, and their direct impact on the electrochemical performance of the SSB. However, these methods will not be covered in this perspective because we think that they deserve a more comprehensive discussion in a separated manuscript. Readers interested in the application of EIS to the study of interphases in SSBs are invited to consult a recently published review.[128]

4.1. Neutron depth profiling (NDP).

In NDP, a low energy neutron (*n*) interacts with a ^{6}Li atom producing an α (^{4}He) and a triton (^{3}H) particle according to the next equation

$$^6\text{Li} + n \rightarrow {}^4\text{He} + {}^3\text{H}$$

As a result of this first collision, the ^{4}He and ^{3}H particles are released with well-defined energies of 2055 and 2727 keV, respectively. Subsequently, the two ejected particles suffer a number of collisions decreasing their original energies at the moment of their formation. The loss of energy can then be correlated to the initial location of the ^{6}Li atom inside the SSBs. Therefore, a higher decrease in energy involves a deeper position of the buried lithium atom inside the stacked material. NDP measurements on SSBs has been always carried out with the *in situ* or *operando* approach.[129–133] The first study was reported by P. H. L. Notten and coworkers.[129] They successfully tracked the diffusion of Li between the cathode and the anode in a $LiCoO_2$ (LCO)/LiPON/Cu microbattery. Interestingly, quantification of (des)inserted Li was in agreement with the charge calculated from the electrochemical cycling curve.

NDP technique has been proved to be very useful in the evaluation of Li transport dynamics during consecutive plating and stripping cycles in Li/solid electrolyte/Li symmetrical cells. The formation and growth of Li dendrites at interfaces has been particularly addressed. In this context, C. Wang *et al.* have recently found by *in situ* NDP experiments that detrimental Li plating can occur inside the bulk solid electrolyte instead the Li electrode/solid electrolyte interface in Li/$Li_7La_3Zr_2O_{12}$/Cu and Li/Li_3PS_4/Pt solid-state cells. The subsequent growth of the Li deposits leads to failure of the battery due to short-circuit. Li plating inside the electrolyte is attributed to the residual but no negligible electronic conduction of $Li_7La_3Zr_2O_{12}$ ($\sigma_e = 5.5 \times 10^{-8}$ S cm^{-1} at 30 °C) and Li_3PS_4 ($\sigma_e = 2.2 \times 10^{-9}$ S cm^{-1} at 30 °C). In contrast, LCO/LiPON/Cu microbatteries does not show any sign of Li deposition inside the solid electrolyte, as LiPON has an extremely low ionic conductivity ($\sigma_e = 10^{-15} – 10^{-12}$ S cm^{-1}). Therefore, this paramount study suggests that electronic conductivity of solid electrolytes is a critical parameter for the cycling life of SSBs, which is rarely reported. Interestingly, a recent *operando* optical microscopy experiment on a NMC 622/LPS/Li battery suggests that Li plating inside the solid state electrolyte occurs before the growth of dendrites at the Li/LPS interface.[70]

Despite the great capacity of *in situ* NDP to monitor Li transport phenomena, particularly at interfaces, this technique shares a fundamental limitation with *in situ* (S)TEM experiments. The analysed SSBs must contain uniform materials and flat surfaces as found in microbatteries. Furthermore, the sampling depth of the technique is usually lower than 50 μm. Thus, devices comprising composite electrodes or solid electrolytes oriented to e-mobility and grid storage cannot be probed.

4.2.X-ray computed tomography (X-CT).

Micro- and nano-X-ray computed tomography (X-CT) is an attractive method enabling the visualization and evaluation of the microstructure of materials in SSBs. Briefly, in X-CT, the assembled SSB is mounted on a sample holder rotating around an axis perpendicular to an incident X-ray beam. 2D transmission X-ray images are then taken at different angles and subsequently combined to generate a 3D image with the aid of digital geometry processing software. Although laboratory-scale instruments exist, the use of synchrotron radiation as X-ray source allows attaining spatial resolutions in the order of 100 nm, which is better than in laboratory instruments (around 1 μm under the best conditions). A comparison of the main features for the two approaches has been recently published for a liquid Li ion battery with a silicon anode.[87]

Contrasts in images acquired by X-CT are the result of differences in X-ray attenuation coefficients between chemical elements, thus light elements displaying a low X-ray absorption, like carbon and Li, are hardly distinguished in the rendered images. This aspect limits the information on interfaces obtained by X-CT. Nevertheless, this technique is probably the most powerful one to unravel the electromechanical dynamics of materials and interphases in SSBs with the advantage that batteries comprising composite electrodes and solid electrolytes can be analysed. The detailed description of the microstructure of composite electrodes and its evolution during cycling is receiving a justified increasing attention since it has been less explored than other phenomena in SSBs.[83,134] X-CT can shed light on this overlooked and important aspect for the electrochemical performance and stability of the device. For instance, J. Janek *et al.* examined the structural changes induced after the first charge in a LCO/$Li_{10}GeP_2S_{12}$/$InLi_x$ SSBs without external compressive pressure by *ex situ* X-CT.[135] It was shown that volume expansion of the negative electrode led to bending of the $Li_{10}GeP_2S_{12}$/$InLi_x$ interface and the whole cell. Furthermore, the formation of cracks was evident at the edges of the battery. Curiously, the stain imposed by volumetric changes produces a beneficial effect: the densification of the solid electrolyte (decrease of porosity from 5.5 % before charging to 2.6 %).

A comprehensive review of all the X-CT experiments conducted on SSBs is out of the scope of this perspective and they would deserve a detailed discussion in a separated manuscript. Thus, only some representative and relevant X-CT experiments will be discussed in this section.

A significant number of X-CT studies has been devoted to research on symmetric Li/solid electrolyte/Li cells. In this context, the group of Nitash Balsara has carried out extensive efforts aimed at elucidating and mastering the growing of Li dendrites and protrusions in symmetric cells containing a rigid polystyrene-block-poly(ethyleneoxide) (PS-b-PEO) block copolymer blended with LiTFSI salt.[136–140] Probably, the most fascinating finding extracted from their synchrotron-based X-CT experiments is the clear observation of the formation of Li protrusions from crystalline impurities inside the Li metal electrode. The formation of dendrites has been traditionally attributed to uneven Li deposition at the Li electrode/solid electrolyte interfaces. However, the results obtained by Balsara *et al.* suggest that Li protrusions and dendrites start in crystalline impurities, probably electronically isolators like Li_2O and Li_3N, initially buried in the bulk of the Li electrode, beneath the electrode/solid electrolyte interface. This observation is extremely relevant as efficient suppression of dendritic structures could be only possible with Li electrodes featuring high purity. This aspect is commonly overlooked in the literature on SSBs. Furthermore, Balsara *et al.* examined the effect of Li salt concentration, temperature and current intensity on the geometry and morphology of dendrites and protrusions.

All the experiments described above were performed *ex situ*. Notwithstanding, numerous *in situ* and *operando* X-CT measurements have also been reported. For instance, M. T. McDowell and coworkers exploited the *in situ* approach to assess the evolution of the microstructure of the solid electrolyte in a Li/$Li_{1+x}AlxGe_{2-x}(PO_4)_3$(LAGP)/Li symmetric cell.[141] Despite the noticeable formation and growing of an interphase layer between the electrodes and the solid electrolyte, it was shown that the formation, propagation and widening of microcracks was responsible for the failure of the cell.

The evolution during cycling of the microstructure of composite electrodes has also been successfully probed by *in situ* and *operando* X-CT.[142,143] An interesting example has been published by Yuta Kimura and coworkers. They combined synchrotron X-CT and X-ray absorption near edge structure (XANES) spectroscopy to evaluate *operando* the 3D spatial distribution of the state of (dis)charge (SOC) of LCO particles in a composite electrodes containing $Li_{2.2}C_{0.8}B_{0.2}O_3$ (LCBO) as solid electrolyte without the presence of conductive additives.[144,145] The analysis of a volume comprising the full thickness of the composite electrode (ca 50 μm and ca 500 x 500 μm edges) revealed a heterogeneous distribution of SOCs. The SOC maps after charge and discharge points out a less efficient delithiation or lithiation, respectively, of LCO particles embedded in the centre of agglomerates of active material particles. The authors propose that this phenomenon is due to poor ionic conductivity at LCO/LCO particles interfaces.

A comparison of the volume probed by the study of Kimura *et al.* and the typical one analysed by common Ga^+ FIB-SEM tomography (see section 3.2.2.1) evidences one of the advantages of X-CT regarding FIB-SEM tomography: the volume of probed material is significantly larger, thus the obtained results should be more representative. Additionally, X-CT is a non-destructive sample method and, consequently, it can be implemented with *operando* and *in situ* spectroelectrochemical measurements. Another advantage consists in the time

required for the analysis of the sample. FIB-SEM tomography involves sequential steps of FIB sectioning and microspic/spectroscopic analysis and, thus, it can be a very time-consuming methodology. In contrast, a full CT-XANES measurement at diverse wavelengths reported by Kimura *et al.* took approximately 35 minutes (one single image at a fixed wavelength took only 26 seconds). The main limitation of CT-XANES stem from the reduced chemical information accessible for this technique. Conversely, the surfaces sequentially exposed in FIB-SEM tomography can be probed with a wide range of microscopic and spectroscopic techniques providing comprehensive chemical information like ToF-SIMS.[146,147] A second drawback of the technique relies on the difficulty to distinguish light elements and voids as it was stated above.

4.3. Nuclear magnetic resonance (NMR).

Li has two stable isotopes with non-zero nuclear spin number (*I*): ^{6}Li (*I* = 1, 7.42 % abundance) and ^{7}Li (*I* = 3/2, 92.58 % abundance).[148] This property has made NMR experiments on ^{6}Li and ^{7}Li nucleus a valuable tool to assess the diffusion and distribution of Li^+ and, in some cases, Li metal at interfaces. In the context of interfacial studies in SSBs, NMR experiments are obviously carried out in the solid state. A description of the particularities of solid state NMR (ssNMR) and the main techniques used in this spectroscopic approach is out of the scope of the present perspective. We will only provide a short explanation of the information that can be extracted from a particular technique when pertinent. Readers interested in getting a deeper knowledge on the principles and main methodologies in ssNMR[149,150] and/or their application to energy storage devices[151] are invited to consult the cited reviews. In the context of interfacial studies on SSBs, NMR measurements have only been performed *ex situ* to the best of our knowledge.

The rate of spontaneous exchange of Li^+ at solid/solid interfaces is a critical parameter for the performance of the battery. However, quantification of this process cannot be carried out with the techniques discussed so far. Alternatively, NMR appears as a valuable tool to extract kinetic parameters associated to Li^+ exchange at interfaces. This information can be gathered from experiments based on the transfer of magnetisation between two Li sites featuring distinguishable chemical shifts (δ). In the absence of strong dipolar interactions between the two nearby Li nuclei, this transfer arises from the spatial diffusion of Li^+ between the two sites. Since the amount of transferred magnetisation is integrated at different times and the experiments can be performed at several temperatures, the self-diffusion coefficient and the activation energy for the spontaneous Li^+ exchange can be calculated under the assumptions of a model derived from the Fick's law. This approach is commonly known in the literature as 2D-EXSY measurements.

The group of Marnix Wagemaker has exploited 2D-EXSY measurements to study spontaneous Li^+ exchange at Li_6PS_5X (X = Cl, Br)/Li_2S [152,153] interfaces. Interestingly, the activation energy for the process at uncycled batteries was found to be low (0.12 and 0.13 eV for interfaces involving Li_6PS_5Cl and Li_6PS_5Br respectively), meaning that Li transport at these interfaces is relatively facile. However, diffusion of Li^+ at the interface is slow as the Li^+ self-diffusion coefficient ($\sim 10^{-11}$ cm^2 s^{-1}) is lower than the same parameter in the bulk of the solid electrolyte ($\sim 10^{-9}$ cm^2 s^{-1}). Thus, limitation of Li^+ transport over the solid electrolyte/active material interface was attributed to a small contact area between the two phases as Li^+ crossing is not energetically hampered. The same group also analysed the spontaneous Li^+ exchange at the Li_6PS_5Br/Li_2S interface after galvanostatic cycling.[153] The application of only two full charge/discharge cycles led to a significant increase of activation energy from 0.13 to 0.39 eV. It was suggested that contact loss between the two phases due to repeated Li_2S volumetric changes and/or formation of interphases could account for this increment.

2D-EXSY has also been exploited to assess the impact of the space charge layer on the Li diffusion resistance at the solid electrolyte/active material interface. To this end, the NASICON-type $Li_{1.5}Al_{0.5}Ge_{1.5}(PO_3)_4$ (LAGP)[154] solid electrolyte was blended, in three different experiments, with three distinct $Li_xV_2O_5$ samples (a common cathode active material) exhibiting diverse Li chemical potential as a consequence of the different degree of lithiation. Hence, LiV_2O_5 presented the same Li chemical potential than LAGP and it did not result in the formation of a space charge layer, while $Li_2V_2O_5$ and $Li_{0.2}V_2O_5$ had lower and higher, respectively, Li chemical potential than LAGP and led to the growing of a space charge layer. The Li exchange NMR measurements revealed the detrimental effect of the space charge layer in the Li transport resistance. The measured activation energy increased from 0.32 eV for the space charge layer free LAGP/LiV_2O_5 interface to 0.52 eV for the LAGP/$Li_2V_2O_5$ interface Therefore, this work suggests that the formation of the space charge layer could have a strong negative impact on the power capability of SSBs.

Li^+ diffusion over grain boundaries inside solid electrolyte is another critical property in SSBs which has been tackled with 2D-EXSY measurements. Wagemaker *et al.* have estimated the kinetics of this process by mixing two similar argyrodites solid electrolytes: Li_6PS_5Cl and Li_6PS_5Br.[155] Since the Li environments in the two materials gave signals with well-separated chemical shifts, Li exchange NMR measurements could be made to quantify its diffusion across the Li_6PS_5Cl/Li_6PS_5Br interface. Although this experiment cannot be properly considered as an evaluation of Li^+ diffusion through grain boundaries of a single material, it is a clever and good approximation. The calculated activation energy of the spontaneous Li^+ exchange was 0.27 eV, which is similar to the value obtained with other NMR analysis based on spin-lattice relaxation.

Li exchange experiments are excellent tools to study composite solid electrolytes containing Li^+ conductive inorganic filler as the promise of improvement of ionic conductivity in these systems versus the fully polymer electrolyte relies on the fast transfer of Li^+ between the polymer and the inorganic phases. Indeed, the efficiency of this exchange is nowadays a source of controversy.[156–158] A remarkable example of the application of 2D EXSY techniques to evaluate Li diffusion across the organic/inorganic interface in composite electrolytes has been recently published by López del Amo and coworkers.[159] The analysed electrolyte consisted in a mixture of PEO:LiTFSI(20:1) and 10 vol% LLZO. The experiments confirmed the spontaneous Li^+ exchange between polymer, LLZO and a layer of LiOH covering the surface of LLZO which is formed due to the

sensitivity to moisture of this material. However, the calculated rate for Li diffusion are low compared to the value roughly estimated from electrochemical impedance measurements. Thus, Li^+ conduction for this solid electrolyte must occur only through the polymer phase.

Although Li 2D-EXSY is probably the most powerful technique to quantify the kinetics of Li diffusion at interfaces, it is not exempt of some limitations. Firstly, the two Li environments in the two phases involved in the exchange should result in chemical shifts sufficiently separated[155] or marked difference in spin-lattice relaxation times.[152] López del Amo and coworkers have shown that discrimination between two close Li signals can be notably improved by application of a ^1H–$^{7\ or\ 6}Li$ cross polarization step previous to the 2D-EXSY sequence. The second limitation concerns the spin-lattice relaxation time as this parameter determines the longer exchange time that can be probed. The spin-lattice relaxation time decreases in the presence of paramagnetic ions; thus it can make challenging the study of Li exchange at interfaces involving common active materials like LCO or NMC. Finally, experiments are carried out ex-situ. This can introduce a source of misinterpretation when the spontaneous Li exchange of a solid electrolyte with an active material at different state of charges is studied. The sample preparation requires disassembling of the battery and recovery of the composite electrode or chemical lithiation of the active material followed by blending and gridding with the solid electrolyte.

Another interesting application of solid-state NMR to the study of interfaces in SSBs is the tracking of formation and growing of Li dendrites by ^7Li magnetic resonance imaging (MRI). For instance, Clare P. Grey *et al* have used this technique to detect and visualise the onset and evolution of this Li microstructures in a $Li/Li_{6.5}La_3Zr_{1.5}Ta_{0.5}O_{12}$(LLZTO)/Li symmetric cell.[160] The stark difference in chemical shift between ^7Li environments in the bulk metal and LLZTO allowed the unambiguous localisation of each phase, including dendritic Li, in the device. Importantly, the experiments revealed the growing of Li microstructures on the surface of the Li metal electrodes, probably corresponding to dendrites, before any sign of degradation in the voltage-time curves during galvanostatic cycling of the system. Furthermore, it was shown that the growing of dendrites occurred simultaneously on the plated and stripped lithium electrodes. The unexpected formation of Li microstructures on the stripped electrode was ascribed to roughing of the surface due to uneven Li releasing and subsequent formation of hot spots exhibiting enhanced current densities.

Despite ^7Li MRI is an attractive tool to monitor and visualise the growing of detrimental Li microstructures such as dendrites, the technique presents a poor spatial resolution (300 μm in above the experiments). This is the reason why the system studied by Clare P. Grey *et al* comprised a solid electrolyte with a thickness of 2.5 mm, which is unpractical from the point of view of energy density.

4.4.Other techniques.

In this section, several techniques with large SDs and less explored for the analysis of interfaces in SSBs will be discussed. Bun Tsuchiya and coworkers have recently developed[161] a new method based on the bombardment of thin SSBs with a beam of O^{4+} ions and high-energy elastic recoil ion-beam detection (ERD) to track *in situ* the evolution of the concentration of Li, and eventually H, at the diverse interfaces in an $LCO/Li_{1.4}Al_{0.4}Ge_{0.7}Ti_{0.9}P_3O_{12}$ (LATP)/Pt microbattery. It was evidenced that charging leads to Li depletion at the $LiCoO_2$/LATP interface and formation of a space charge layer with a 120 nm thickness in the solid electrolyte. The limitations of this approach are similar to that found in NDP: batteries with small dimensions, i.e. microbatteries, and well-defined and flat surfaces can only be analysed. Therefore, experiments cannot be conducted on composite and thick solid electrolytes and electrodes.

In variable energy hard X-ray photoelectron spectroscopy (VE-HAXPES), the energy of a synchrotron light source can be tuned (3 – 8 keV) to increase the inelastic mean free path (IMFP) of photoelectrons.[162] As a consequence, the detection depth of HAXPES is significantly larger than in XPS experiments carried out in common laboratory XPS instruments, which usually use Al Kα = (1486.7 eV) as X-ray source. Xueliang Sun et al. used VE-HAXPES to evaluate the formation and thickness of interphases in three different layered materials relevant in the SSBs research field: LATP/LCO, LATP/Al_2O_3/LCO and LATP/Li_3PO_4/LCO. In the two last configurations, Al_2O_3 and Li_3PO_4 played the role of a buffer material aimed at preventing interfusion of elements between the LATP and LCO layers. The combination of several techniques including VE-HAXPES indicated that Li_3PO_4 was the most effective buffer material.

In situ and *operando* HAXPES measurements on a cycling LCO/ $Li_{1+x+y}Al_x(Ti, Ge)_{2-x}Si_yP_{3-y}O_{12}$ (LASGTP)/Li microbattery have been also carried out recently.[163] Hard X-ray enabled recording the core-level XPS spectra for several elements in a thickness region comprising the Al (current collector)/LCO/LASGTP interfaces. Similarly to the *operando* XPS experiments with a conventional laboratory instrument reported by the group of Mario El Kazzi,[66–68] a shift in the binding energy of peaks associated to the solid electrolyte was observed while the position of the Al 1s peaks of the current collector (grounded to the analyser) remained unchanged. Surprisingly, the O 1s peak corresponding to the lattice oxygen from LCO splitted into two peaks after charging. Hence, the authors suggested a participation of oxygen anions in the redox activity of the active material. Although Mario El Kazzi *at al.* studied also LCO as active material in their first contribution,[66] they did not provide unfortunately O 1s core-level spectra to allow for comparison with this stunning finding.

Despite the increased depth detection provided by HAXPES vs laboratory XPS, the value is insufficient to be considered as a bulk technique for conventional SSBs. Sampling depths in HAXPES can attain 20-30 nm, which is extremely thin as compared with the thickness of common composite electrodes (40 – 100 μm) for applications in e-mobility or grid storage. However, we have preferred to discuss HAXPES in the framework of the bulk approach as most applications of this technique in the field of SSBs aim at developing a non-destructive method which avoids also the modification of the current collectors.

Another challenge in HAXPES concerns the decrease of the X-ray cross-sections of elements with an increase of the wavelength of the X-ray source.[164] Indeed, this is one of the main reasons why HAXPES is commonly carried out with synchrotron X-ray sources featuring a high brightness. A quick insight of the effect of X-ray energy on the quality of XPS data can be gathered from the aforementioned experiments reported by Xueliang Sun *et al.* using VE-HAXPES.[162] Finally, since a highly bright source is mandatory to obtain spectra with good quality in HAXPES, it remains to be proved if these X-ray sources do not lead to degradation of sensitive materials contained in SSBs like Li metal, organic polymers and Li salts.

5. A note of warning: depth profiling based on the use of ion etching.

Currently, the most popular approach to analyse buried interphases by XPS and TOF-SIMS is ion etching in the analysis chamber. Briefly, the procedure relies on the sequential repetition of sputtering a layer of surface material by an ion beam and subsequent analysis of the newly created surface by one of the two techniques. This approach enables the construction of a depth profile in which the composition of a hetero-layered material can be resolved. Unlike BIB polishing (section 3.1.1.3), the ion gun for depth profiling impinges directly on the sample with a higher angle of incidence (typically between 45° - 60°) creating a crater larger than the analysis spot. The most common ion beam employed until now is based on energetic Ar^+ plasma.

Nowadays, depth profiling is widely in the analysis of interphases in batteries to gain access to the spatially-resolved chemical composition of solid electrolyte interphases (SEIs) and cathode electrolyte interphases (CEIs).[165] The first documented study of the implementation of Ar^+ ion etching to study buried interfaces in the context of SSBs dates back to 2001 and it was carried by Masayoshi Watanabe and coworkers.[28] In their contribution, the SEI formed on a Li foil after prolonged contact (>1 month at 60°C) with a polymer solid electrolyte, made of cross-linked mono-acrylated and tri-acrylated copolymers of ethylene oxide and propylene oxide blended with LiTFSI, was analysed by XPS depth profiling. The spectra taken at increasing etching times unravelled a tri-layered SEI in which the outermost layer consists in a mixture of organic components (polymer residues and decomposition products from Li salts) and a minor amount of LiF, the intermediate layer is mainly made of Li_2CO_3 or LiOH and LiF, and the inner layer contains a mixture of Li_2O and LiF.

In this perspective, we provide experimental results assessing common interpretations of depth profiling studies based on ion etching to define spatially the chemical composition of interphases in Li ion and solid-state batteries. In our study, the stability under the ion beam of one highly popular solid electrolyte polymer film (PEO + LiTFSI) was evaluated. The surface of the film was initially irradiated for 10 s with an Ar^+ beam at room temperature (298 K) similar to the one used previously by the group of Watanabe and in most of literature reports (**Figure 9**, upper). Despite the short duration of the ion etching step, the chemical state of the components of the film is severely affected. As it could be expected, the C 1s core XPS spectrum evidence the formation of degradation products containing an increasing amount of *C*-*C*(H) (≈ 285 eV) and probably a mixture of $C(H)_x$-F_y and *C*-O_x bonds (small signals between 287.5 - 291.5 eV). Importantly, the F 1s core spectrum shows the formation of an important amount of LiF (684.5 eV) as decomposition product. The origin of LiF is probably an ion induced degradation reaction of the LiTFSI salt. Therefore, depth profiling by Ar^+ etching on buried interphases in SSBs can lead to the misinterpretation of a hetero-layered material comprising an outermost layer made of an organic-rich phase, actually corresponding to the no sputtered surface which has not been degraded, and an inner and more inorganic layer rich in LiF, actually corresponding to the degradation of the Li salt after sputtering of the material. Furthermore, certain inorganic compounds also suffer from chemical instability when exposed to Ar^+ beams. This is the case for Li_2CO_3 and LiOH, which are commonly found in SEIs and CEIs, and are known to partially convert into Li_2O.[166,167] Thus, the presence of Li_2O as an inherent and inner component of interphases can also be critically discussed if this information was gathered from Ar^+ ion etching. In order to prevent the deleterious reactions triggered by Ar^+ etching, we envisaged two different potential solutions. Firstly, the temperature of the process was reduced (143 K). This approach had a negligible beneficial effect suggesting that the degradation reaction is induced by the formation of free radicals intermediates and it is not only a result of the low electronic and thermal conductivities of organic materials (**Figure 9**, bottom).[168]

In a second strategy, the etching was carried out under more gentle conditions by using an argon gas cluster ion beam (GCIB). This strategy has been successfully applied to the surface analysis of sensitive organic layered materials in the field of photovoltaics.[169] Indeed, the use of GCIB at both room (**Figure 9**, upper) and low (**Figure 9**, bottom) temperatures reduces the degradation of the PEO:LiTFSI film as the intensity of the peaks associated to decomposition products in the C 1s core spectra are significantly lower and the intensity of the peak associated to PEO is almost constant. Notwithstanding, inspection of the F 1s core spectra reveals the unambiguous formation of LiF after sputtering. Therefore, LiTFSI is also degraded under these conditions, although in a lesser extent when compared to Ar^+ experiments.

Since etching rates (nm s^{-1}) are significantly slower with GCIBs than with Ar^+ beams and inorganic materials are hardly sputtered with GCIBs, there is thus no clear advantage in using GCIBs for depth profiling in SSBs containing LiTFSI salt or a mixture of inorganic and organic materials. Moreover, considering the degradation phenomenon under Ar^+, depth profiling using Ar^+ ion etching should not be performed without caution for such inorganic/organic composites.[28,29,116,170]

Conclusions

The performance of current SSBs is dictated by the electro-chemo-mechanical phenomena occurring at the interfaces of materials. Hence, the comprehensive understanding of these processes is vital to advance toward the development of commercially available SSBs. However, the buried nature of the interfaces makes difficult the acquisition of reliable results by common spectroscopic and microscopic techniques. This critical aspect is usually circumvented in the increasing number of reports on interfacial studies in SSBs. Indeed, from the perspective of interfacial studies, the buried nature of interfaces in SSBs is the critical difference with the same kind of analysis in traditional Li-ion batteries (LIBs) containing liquid electrolytes. In LIBs, the cathode/separator/anode assembly can be relatively easily separated without compromise the structural integrity and chemical composition of interphases. Although, even in this devices, there can be controversy about certain manipulations, e.g. the suitability of rinsing the electrodes after disassembling of the cell.[171] Performing the same separation strategy in SSBs is not convenient for the reasons explained in section 1. Furthermore, if the cathode/solid electrolyte/anode assembly can be easily separated in a SSB, it means that interfacial contact in the system is poor and the observed reactivity could be actually mitigated regarding a battery with better interfacial contacts which is more representative of the intrinsic reactivity of the materials.

Despite the more challenging character of analysis of interfaces in SSBs, the solid state of all the components of these systems makes easier the development of *in situ* and *operando* methods under ultra-high vacuum conditions. In LIBs, the application of this kind of techniques is obviously more difficult due to the evaporation and stability of the liquid electrolyte. For instance, *in situ* XPS experiments have been carried out on LIBs, but the batteries comprised an ionic liquid electrolyte stable under high vacuum conditions and a specially conceived Li permeable amorphous carbon membrane.[172–174] Therefore, SSBs present the advantage of simple *in situ* and *operando* compatibility with very powerful characterization techniques (TEM, SEM, XPS, ToF-SIMS among others).However, as thoroughly discussed in this perspective, careful sample preparation procedures must be adopted to ensure the reliability and reproducibility of the results.

In this perspective, we have evaluated the two main approaches employed nowadays to tackle the challenge of achieving reliable, reproducible and representative information from buried interfaces in SSBs. Likewise, excellent examples illustrating the strength of these approaches to extract valuable electro-chemo-mechanical interfacial data have been discussed. Furthermore, it has been shown that the implementation of robust procedures to get access and analyse buried interfaces has paved the way to the development of *in situ* and *operando* measurements.

In **Table 1**, we compile the advantages and drawbacks of all the methodologies used in each approach following criteria from a

ARTICLE

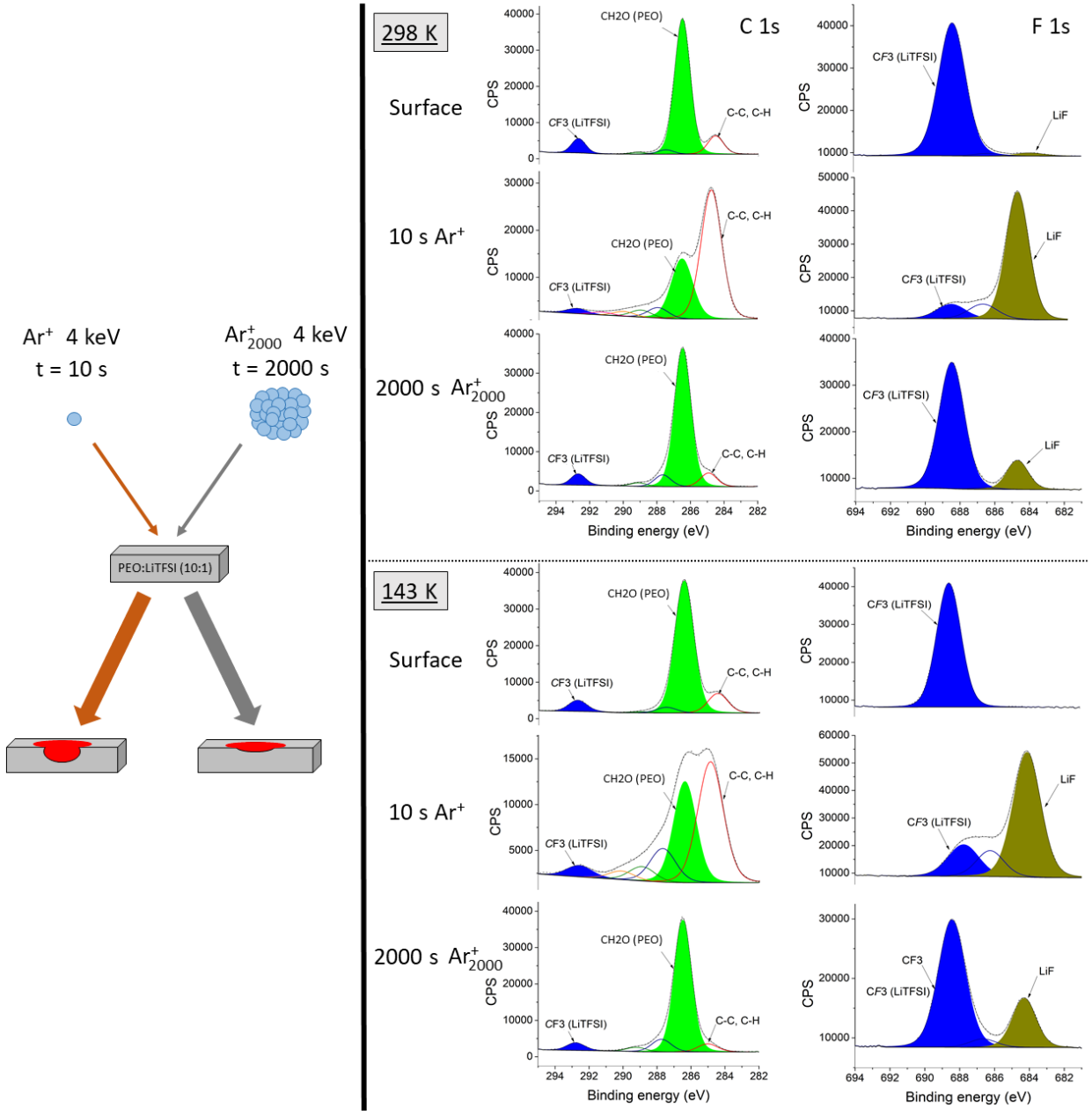

Figure 9. Depth profiling study on a PEO:LiTSFI (10:1) film using Ar^+ at 4 keV or Ar^+_{2000} at 4 keV (2 eV per Ar atom) as sputtering beam. The experimental data is represented by dots and the fitting line results from convolution of the proposed components.

sample preparation outlook, namely the level of sample destruction, the compatibility with certain materials and SSBs, the risk of degradation of sensitive materials, the adaptability to *in situ*/*operando* experiments and the dimensions of the analysable area for procedures involving exposing cross-sections. In **Table 2**, a different perspective is considered. Thus, the advantages and drawbacks for the diverse analytical techniques more frequently used in *the Uncovering approach* and the methods of *the bulk approach* are assessed from analytical criteria such as lateral resolution, level of extracted chemical information or possible degradation of materials due to analytical beam-sample interaction.

Table 1. Resume of advantages and drawbacks for the uncovering and bulk approaches considering aspects associated to the preparation of samples from SSBs and the key features of the prepared samples.

Approach	Methodology/technique	Advantages	Drawbacks
Uncovering buried interfaces	(Cryo)Microtomy	• Fast • Creation of large cross-sections • Simple procedure to prepare samples for *in situ* and *operando* experiments	• Significantly destructive • No assured preservation of microstructure even under cryogenic conditions • Only used for SSBs with polymer solid electrolyte until now
	FIB	• Less destructive than (cryo)microtomy and BIB polishing • Best procedure for preparation of extremely thin cross-sections for (S)TEM-EELS analysis • Combined with a number of microscopic and spectroscopic techniques: (S)TEM-EELS, SEM, ToF-SIMS. • Only method allowing the preparation of nanobatteries from microbatteries for *in situ* and *operando* experiments	• Creation of small cross-sections (50 μm × 50 μm). Although enlarged with Xe plasma beam • Produce damage in the created surface (minimized if carried out under cryogenic conditions and/or combined with a final low-energy polishing step) • Preservation of the microstructure of certain materials only possible under cryogenic conditions, e. g. Li electrodes • Complex procedure for preparation of nanobatteries for *in situ* and *operando* experiments • Impossible application on composites electrodes and solid electrolytes for *in situ* and *operando* experiments
	BIB polishing	• Preparation of large cross-sections (ca 700 μm width x 400 μm depth) • Combined with a number of microscopic and spectroscopic techniques: SEM, AES-SAM, ToF-SIMS, cAFM, SSRM, KPM, RAMAN. • Allowing for the preparation of samples for a great variety of *in situ* and *operando* experiments (*in situ* less complex than for FIB) • Possible application on composites electrodes and solid electrolytes for *in situ* and *operando* experiments	• More destructive than FIB, but less than (cryo)microtomy • Produce damage in the created surface due to heating effects on thermally insulating materials like polymers. (minimised if process carried out under cryogenic conditions) • Exposed cross-section less reactive than the bulk in *in situ* and *operando* experiments (edge effect)
	Perforated current collectors	• Non-destructive • Excellent for the preparation of samples for *in situ* and *operando* XPS and sXAS experiments, where spatial resolution or sensitive are an issue • Possible application on composites electrodes and	• More difficult composite electrode processing due to casting or pressing of materials on a perforated current collector • Induction of a non-homogeneous distribution of the electrical field

		solid electrolytes for *in situ* and *operando* experiments	• Exposed interfaces only inside the composite cathode and near the current collector
Bulk techniques	NDP	• Non-destructive • Particularly adapted to *operando* experiments	• Only adapted to batteries with flat and well-defined interfaces (mainly microbatteries) • Non-conventional instrumentation
	Micro and nano X-CT	• Non-destructive • Compatible with *in situ* and *operando* experiments	• Special design of cells for *in situ* and *operando* experiments to optimise detection of signal
	Solid state NMR	• Non-destructive for solid electrolyte study • Conventional instrumentation	• Destructive for full battery study • Only *ex-situ*
	O^{4+} bombardment and ERD	• Non-destructive • Particularly adapted to *in situ* experiments	• Only adapted to batteries with flat and well-defined interfaces (mainly microbatteries) • Non-conventional instrumentation
	HAXPES	• Non-destructive • Compatible with *in situ* and *operando* experiments	• Only considered bulk technique with microbatteries containing flat and well-defined interfaces

Table 2. Resume of advantages and drawbacks for the uncovering and bulk approaches considering aspects associated to the analytical measurement of samples.

Approach	Technique	Advantages	Drawbacks
Uncovering buried interfaces	SEM + (EDS)	• Good lateral resolution • Information on microstructure of materials in 2D an even 3D when combined with FIB (FIB tomography)	• Limited chemical information on interphases • Obtained chemical information by EDS no representative of the chemical state of cross-section surface (large SD) • E-beam damage of organic materials and Li
	(S)TEM + (EELS, EH)	• Excellent lateral resolution • Li detection possible with EELS • Probing of electric fields possible with EH	• Limited chemical information on interphases • E-beam damage of organic materials and Li • Limited to the study of extremely thin samples (< 100 nm) • *In-situ* and *operando* experiments restricted to nanobatteries
	XPS	• Rich chemical information on interphases • Possibility of probing differences in electric potentials, particularly in *in situ* and *operando* experiments	• Poor lateral resolution • Challenging for Li detection • Ambiguous interpretations when combined with depth profiling

		• Limited degradation of materials due to x-ray beam	
	ToF-SIMS	• Good lateral resolution • Good chemical information on interphases • Best technique for Li detection	• Incompatible with *operando* experiments • Need of polishing during *in situ* experiments • Ambiguous interpretations when combined with depth profiling
	SPM	• Excellent lateral resolution • Determination, at the nanometre level, of parameters inaccessible with other conventional techniques, e.g. electric potential and resistance.	• No chemical information on interphases • Extremely sensitive to the flatness of the surface
	AES and SAM	• Excellent lateral resolution • Good sensitivity for Li detection • Information on microstructure of materials in 2D	• Limited chemical information on interphases • E-beam damage of organic materials and Li
	RAMAN	• Good lateral resolution	• Challenging chemical interpretation of signals from interphases • Adventitious degradation of materials, particularly organics, due to laser heating
	OM	• Simple • Information on microstructure of materials in 2D • No degradation of materials • Particularly adapted to *operando* experiments	• Limited lateral resolution • No chemical information on interphases
	sXAS	• Best technique to probe metals oxidation states • Limited degradation of materials due to x-ray beam	• Limited lateral resolution • No chemical information on interphases
Bulk techniques	NDP	• Good lateral resolution • Allow assessing the distribution of Li in the battery • No degradation of materials • Particularly adapted to *operando* experiments	• Limited sampling depth (< 50 μm) • No chemical or structural information on interphases

	Micro and nano X-CT	• Good spatial resolution with x-ray synchrotron radiation (up to 50 nm) • Good sampling depth (mm scale) • Information on 3D microstructure of materials • Provide insight of transition metals oxidation states at variable x-ray energy experiments	• Reduced spatial resolution in lab-scale instrument (ca 1 μm) • No chemical information on interphases • Challenging distinction between critical light elements in SSBs, like C *vs* Li, and light elements *vs* voids
	Solid state NMR	• Quantification of Li exchange kinetics • No degradation of materials	• Limited to Li study • Extremely poor spatial resolution for MRI (300 μm)
	O^{4+} bombardment and ERD	• Good spatial resolution (< 100 nm) • Allow assessing the distribution of Li and H in the battery • No degradation of materials • Particularly adapted to *in situ* experiments	• Limited sampling depth (< 200 μm) • No chemical information on interphases
	HAXPES	• Rich chemical information on interphases • Possibility of probing differences in electric potentials, particularly in *in situ* and *operando* experiments	• Limited lateral resolution • Extremely limited sampling depth (< 30 nm) • Challenging for Li detection • Risk of x-ray beam degradation of sensitive materials like polymers and Li salts.

Finally, we have examined with new experiments carried out in our laboratory the suitability of depth profiling studies to unveil and spatially resolve the chemical composition of interphases in SSBs containing a blend of polymer and Li salt as electrolyte. Our results suggest that extreme precaution must be adopted to interpret the data as polymers and Li salts are sensitive to the ion milling beam even with soft GCIBs and low operation temperatures (143 K). Since organic molecules and residual amounts of Li salt are common components of the SEI and CEI in conventional LIBs, similar precautions should be considered in the depth profiling analysis of these samples.

The growing interest in SSBs at both the academic and industrial level is expected to attract increasingly the focus on interfacial phenomena as a key issue to improve the capabilities of the devices. Moreover, buried interfaces are commonly found in materials science. For instance, hetero-layered films in photovoltaics, core-shell nanostructures and anti-corrosion surface coatings. Thus, all the discussed strategies also concern the analysis of a wide range of materials and devices. Similarly, the field of analysis of interfaces in SSBs could adopt techniques and methodologies exploited in LIBs and devices facing the challenge of buried interfaces. For instance, vibrational sum frequency generation (vSFG) spectroscopy is a powerful method that has been exploited in LIBs[175] and other electrochemical devices[176–178] for probing molecular interactions at interfaces. VSFG spectroscopy detects resonant vibrational transitions which are both IR and RAMAN actives. The recorded sum-frequency photon can only be emitted by molecules localised at the interface of two centrosymmetric environments. This particularity makes vSFG spectroscopy a surface-sensitive technique. A more detailed description on the physical principles behind this spectroscopy can be found in the references cited above. In LIBs, vSFG has provided relevant information about the varied orientation that can adopt absorbed solvent molecules on the surface of several active materials like Si anodes[179] and LCO cathodes.[180,181] The application of this analytical tool to the study of interfaces in SSBs could reveal unnoticed molecular interactions, particularly in systems containing organic polymers or composites as electrolytes. For instance, vSFG spectroscopy could be employed to unravel the orientation and interaction of functional groups at the polymer/inorganic filler interface. It is worth nothing that this technique is surface-sensitive, thus it will require rigorous sample preparation procedures.

Neutron computed tomography could be also an attractive technique to track the distribution of Li at interfaces of SSBs, as scattering cross-sections of light elements are enhanced as compared to analogous experiments based on x-ray sources.

Furthermore, neutron computed tomography is sensitive to isotopes, with ^{6}Li and ^{7}Li exhibiting extremely different scattering cross-sections.[182] Preliminary experiments[183] seem validate the application of this analytical tool to delineate a Li profile at the cathode/solid electrolyte interface in a $TiS_2/^{6}Li_3PS_4/In\text{-}^{6}Li$ battery.

To conclude, we expect that our perspective makes researchers scrutinizing materials with buried interfaces aware of the suitability of the chosen methodology to uncover them besides the attainable structural and/or chemical information that can be extracted from a particular analytical technique. Similarly, we encourage researchers interested in the analysis of interfacial phenomena in SSBs to combine the discussed robust methodologies with less explored analytical techniques, like vSFG, to gain deeper insight on electro-chemo-mechanical processes at interfaces.

Conflicts of interest

There are no conflicts to declare.

Acknowledgements

This perspective was carried out as part of the HUB RAISE2024 project. This project has received funding from Excellence Initiative of Université de Pau et des Pays de l'Adour – I-Site E2S UPPA, a French "Investissements d'Avenir" programme.

References

1 R. Chen, Q. Li, X. Yu, L. Chen and H. Li, *Chem. Rev. (Washington, DC, U. S.)*, 2019, **120**, 6820–6877.
2 J. Janek and W. G. Zeier, *Nature Energy*, 2016, **1**, 16141.
3 A. Mauger, C. M. Julien, A. Paolella, M. Armand and K. Zaghib, *Materials (Basel)*, 2019, **12**, 3892.
4 Y. Ding, Z. P. Cano, A. Yu, J. Lu and Z. Chen, *Electrochemical Energy Reviews*, 2019, **2**, 1–28.
5 G. Crabtree, *Science*, 2019, **366**, 422.
6 D. Zhou, D. Shanmukaraj, A. Tkacheva, M. Armand and G. Wang, *Chem*, 2019, **5**, 2326–2352.
7 T. Famprikis, P. Canepa, J. A. Dawson, M. S. Islam and C. Masquelier, *Nat. Mater.*, 2019, **18**, 1278–1291.
8 S. Li, S.-Q. Zhang, L. Shen, Q. Liu, J.-B. Ma, W. Lv, Y.-B. He and Q.-H. Yang, *Advanced Science*, 2020, **7**, 1903088.
9 X. Yu and A. Manthiram, *Energy Storage Materials*, 2020, **34**, 282–300.
10 Y. Zheng, Y. Yao, J. Ou, M. Li, D. Luo, H. Dou, Z. Li, K. Amine, A. Yu and Z. Chen, *Chem. Soc. Rev.*, 2020, **49**, 8790–8839.
11 D. Campanella, D. Belanger and A. Paolella, *Journal of Power Sources*, 2021, **482**, 228949.
12 L. Xu, J. Li, W. Deng, H. Shuai, S. Li, Z. Xu, J. Li, H. Hou, H. Peng, G. Zou and X. Ji, *Advanced Energy Materials*, 2020, **11**, 2000648.
13 D. H. S. Tan, A. Banerjee, Z. Chen and Y. S. Meng, *Nat. Nanotechnol.*, 2020, **15**, 170–180.
14 C. Sångeland, J. Mindemark, R. Younesi and D. Brandell, *Solid State Ionics*, 2019, **343**, 115068.
15 H.-D. Lim, J.-H. Park, H.-J. Shin, J. Jeong, J. T. Kim, K.-W. Nam, H.-G. Jung and K. Y. Chung, *Energy Storage Materials*, 2019, **25**, 224–250.
16 A. Banerjee, X. Wang, C. Fang, E. A. Wu and Y. S. Meng, *Chem. Rev.*, 2020, **120**, 6878–6933.
17 T. A. Wynn, J. Z. Lee, A. Banerjee and Y. S. Meng, *MRS Bulletin*, 2018, **43**, 768–774.
18 T. Chen, L. Zhang, Z. Zhang, P. Li, H. Wang, C. Yu, X. Yan, L. Wang and B. Xu, *ACS Appl. Mater. Interfaces*, 2019, **11**, 40808–40816.
19 A. Y. Kim, F. Strauss, T. Bartsch, J. H. Teo, T. Hatsukade, A. Mazilkin, J. Janek, P. Hartmann and T. Brezesinski, *Chem. Mater.*, 2019, **31**, 9664–9672.
20 H.-J. Guo, H.-X. Wang, Y.-J. Guo, G.-X. Liu, J. Wan, Y.-X. Song, X.-A. Yang, F.-F. Jia, F.-Y. Wang, Y.-G. Guo, R. Wen and L.-J. Wan, *J. Am. Chem. Soc.*, 2020, **142**, 20752–20762.
21 J. Zhang, C. Zheng, L. Li, Y. Xia, H. Huang, Y. Gan, C. Liang, X. He, X. Tao and W. Zhang, *Advanced Energy Materials*, 2020, **10**, 1903311.
22 A. Banerjee, H. Tang, X. Wang, J.-H. Cheng, H. Nguyen, M. Zhang, D. H. S. Tan, T. A. Wynn, E. A. Wu, J.-M. Doux, T. Wu, L. Ma, G. E. Sterbinsky, M. S. D'Souza, S. P. Ong and Y. S. Meng, *ACS Appl. Mater. Interfaces*, 2019, **11**, 43138–43145.
23 J. Liang, S. Hwang, S. Li, J. Luo, Y. Sun, Y. Zhao, Q. Sun, W. Li, M. Li, M. N. Banis, X. Li, R. Li, L. Zhang, S. Zhao, S. Lu, H. Huang, D. Su and X. Sun, *Nano Energy*, 2020, **78**, 105107.
24 R. Schlenker, D. Stępień, P. Koch, T. Hupfer, S. Indris, B. Roling, V. Miß, A. Fuchs, M. Wilhelmi and H. Ehrenberg, *ACS Appl. Mater. Interfaces*, 2020, **12**, 20012–20025.
25 L. Wang, D. Liu, T. Huang, Z. Geng and A. Yu, *RSC Advances*, 2020, **10**, 10038–10045.
26 C. Xu, B. Sun, T. Gustafsson, K. Edström, D. Brandell and M. Hahlin, *J. Mater. Chem. A*, 2014, **2**, 7256–7264.
27 L. Held and S. Schwab, *Significance*, 2020, **17**, 10–11.

28 I. Ismail, A. Noda, A. Nishimoto and M. Watanabe, *Electrochim. Acta*, 2001, **46**, 1595–1603.
29 N. Wu, Y. Li, A. Dolocan, W. Li, H. Xu, B. Xu, N. S. Grundish, Z. Cui, H. Jin and J. B. Goodenough, *Adv. Funct. Mater.*, 2020, **30**, 2000831.
30 S.-Y. Lang, Z.-Z. Shen, X.-C. Hu, Y. Shi, Y.-G. Guo, F.-F. Jia, F.-Y. Wang, R. Wen and L.-J. Wan, *Nano Energy*, 2020, **75**, 104967.
31 J. Auvergniot, A. Cassel, J.-B. Ledeuil, V. Viallet, V. Seznec and R. Dedryvère, *Chem. Mater.*, 2017, **29**, 3883–3890.
32 M. G. Boebinger, J. A. Lewis, S. E. Sandoval and M. T. McDowell, *ACS Energy Letters*, 2020, **5**, 335–345.
33 L. Yang, W. You, X. Zhao, H. Guo, X. Li, J. Zhang, Y. Wang and R. Che, *Nanoscale*, 2019, **11**, 17557–17562.
34 X. Liu, D. Wang, G. Liu, V. Srinivasan, Z. Liu, Z. Hussain and W. Yang, *Nature Communications*, 2013, **4**, 2568.
35 P. P. R. M. L. Harks, F. M. Mulder and P. H. L. Notten, *J. Power Sources*, 2015, **288**, 92–105.
36 H. Masuda, N. Ishida, Y. Ogata, D. Ito and D. Fujita, *Nanoscale*, 2017, **9**, 893–898.
37 M. Otoyama, Y. Ito, A. Hayashi and M. Tatsumisago, *J. Power Sources*, 2016, **302**, 419–425.
38 W. Zhang, F. H. Richter, S. P. Culver, T. Leichtweiss, J. G. Lozano, C. Dietrich, P. G. Bruce, W. G. Zeier and J. Janek, *ACS Appl. Mater. Interfaces*, 2018, **10**, 22226–22236.
39 J. Liu, X. Shen, J. Zhou, M. Wang, C. Niu, T. Qian and C. Yan, *ACS Appl. Mater. Interfaces*, 2019, **11**, 45048–45056.
40 M. Otoyama, T. Yamaoka, H. Ito, Y. Inagi, A. Sakuda, M. Tatsumisago and A. Hayashi, *J. Phys. Chem. C*, 2021, **125**, 2841–2849.
41 H. Masuda, N. Ishida, Y. Ogata, D. Ito and D. Fujita, *J. Power Sources*, 2018, **400**, 527–532.
42 S. Ding, L. Fairgrieve-Park, O. Sendetskyi and M. D. Fleischauer, *Journal of Power Sources*, 2021, **488**, 229404.
43 S. H. Kim, K. Kim, H. Choi, D. Im, S. Heo and H. S. Choi, *Journal of Materials Chemistry A*, 2019, **7**, 13650–13657.
44 S. Randau, D. A. Weber, O. Kötz, R. Koerver, P. Braun, A. Weber, E. Ivers-Tiffée, T. Adermann, J. Kulisch, W. G. Zeier, F. H. Richter and J. Janek, *Nature Energy*, 2020, **5**, 259–270.
45 M. Otoyama, H. Kowada, A. Sakuda, M. Tatsumisago and A. Hayashi, *The Journal of Physical Chemistry Letters*, 2020, **11**, 900–904.
46 K. P. Abhilash, P. C. Selvin, B. Nalini, R. Jose, X. Hui, H. I. Elim and M. V. Reddy, *Solid State Ionics*, 2019, **341**, 115032.
47 J. Auvergniot, A. Cassel, D. Foix, V. Viallet, V. Seznec and R. Dedryvère, *Solid State Ionics*, 2017, **300**, 78–85.
48 S. Kaboli, H. Demers, A. Paolella, A. Darwiche, M. Dontigny, D. Clément, A. Guerfi, M. L. Trudeau, J. B. Goodenough and K. Zaghib, *Nano Lett.*, 2020, **20**, 1607–1613.
49 G. H. Michler, Ed., in *Electron Microscopy of Polymers*, Springer Berlin Heidelberg, Berlin, Heidelberg, 2008, pp. 199–217.
50 J. Z. Au - Lee, T. A. Au - Wynn, Y. S. Au - Meng and D. Au - Santhanagopalan, *JoVE*, 2018, e56259.
51 F. Walther, R. Koerver, T. Fuchs, S. Ohno, J. Sann, M. Rohnke, W. G. Zeier and J. Janek, *Chem. Mater.*, 2019, **31**, 3745–3755.
52 F. Walther, S. Randau, Y. Schneider, J. Sann, M. Rohnke, F. H. Richter, W. G. Zeier and J. Janek, *Chem. Mater.*, 2020, **32**, 6123–6136.
53 F. Walther, F. Strauss, X. Wu, B. Mogwitz, J. Hertle, J. Sann, M. Rohnke, T. Brezesinski and J. Janek, *Chem. Mater.*, 2021, **33**, 2110–2125.
54 J. Z. Lee, T. A. Wynn, M. A. Schroeder, J. Alvarado, X. Wang, K. Xu and Y. S. Meng, *ACS Energy Letters*, 2019, **4**, 489–493.
55 T. L. Burnett, R. Kelley, B. Winiarski, L. Contreras, M. Daly, A. Gholinia, M. G. Burke and P. J. Withers, *Ultramicroscopy*, 2016, **161**, 119–129.
56 R. D. Kelley, K. Song, B. Van Leer, D. Wall and L. Kwakman, *Microscopy and Microanalysis*, 2013, **19**, 862–863.
57 B. Winiarski, *Microscopy and Microanalysis*, 2020, **26**, 2226–2227.
58 Plasma FIB - TESCAN AMBER X, https://www.tescan.com/product/fib-sem-for-materials-science-tescan-amber-x/, (accessed December 17, 2020).
59 R. Jiang, M. Li, Y. Yao, J. Guan and H. Lu, *Front. Mater. Sci.*, 2019, **13**, 107–125.
60 Y. Zeng, Z. Liu, W. Wu, F. Xu and J. Shi, *Microporous and Mesoporous Materials*, 2016, **220**, 163–167.
61 L. Madec, C. Tang, J.-B. Ledeuil, D. Giaume, L. Guerlou-Demourgues and H. Martinez, *J. Electrochem. Soc.*, 2021, **168**, 010508.
62 J. B. Ledeuil, A. Uhart, S. Soule, J. Allouche, J. C. Dupin and H. Martinez, *Nanoscale*, 2014, **6**, 11130–40.

63 A. Uhart, J. B. Ledeuil, B. Pecquenard, F. Le Cras, M. Proust and H. Martinez, *ACS Appl. Mater. Interfaces*, 2017, **9**, 33238–33249.
64 H. Masuda, K. Matsushita, D. Ito, D. Fujita and N. Ishida, *Communications Chemistry*, 2019, **2**, 140.
65 M. J. Smith, T. Schmidt, K. Thompson and M. Dixon, *Herit Sci*, 2019, **7**, 74.
66 X. Wu, C. Villevieille, P. Novák and M. El Kazzi, *Phys. Chem. Chem. Phys.*, 2018, **20**, 11123–11129.
67 X. Wu, C. Villevieille, P. Novák and M. El Kazzi, *Journal of Materials Chemistry A*, 2020, **8**, 5138–5146.
68 M. Mirolo, X. Wu, C. A. F. Vaz, P. Novák and M. El Kazzi, *ACS Appl. Mater. Interfaces*, 2021, **13**, 2547–2557.
69 M. Yamamoto, Y. Terauchi, A. Sakuda, A. Kato and M. Takahashi, *Journal of Power Sources*, 2020, **473**, 228595.
70 M. Sun, T. Liu, Y. Yuan, M. Ling, N. Xu, Y. Liu, L. Yan, H. Li, C. Liu, Y. Lu, Y. Shi, Y. He, Y. Guo, X. Tao, C. Liang and J. Lu, *ACS Energy Lett.*, 2021, **6**, 451–458.
71 S. Kim, C. Jung, H. Kim, K. E. Thomas-Alyea, G. Yoon, B. Kim, M. E. Badding, Z. Song, J. Chang, J. Kim, D. Im and K. Kang, *Advanced Energy Materials*, 2020, **10**, 1903993.
72 Y.-X. Song, Y. Shi, J. Wan, S.-Y. Lang, X.-C. Hu, H.-J. Yan, B. Liu, Y.-G. Guo, R. Wen and L.-J. Wan, *Energy Environ. Sci*, 2019, **12**, 2496–2506.
73 W. Manalastas, J. Rikarte, R. J. Chater, R. Brugge, A. Aguadero, L. Buannic, A. Llordés, F. Aguesse and J. Kilner, *J. Power Sources*, 2019, **412**, 287–293.
74 E. Kazyak, R. Garcia-Mendez, W. S. LePage, A. Sharafi, A. L. Davis, A. J. Sanchez, K.-H. Chen, C. Haslam, J. Sakamoto and N. P. Dasgupta, *Matter*, 2020, **2**, 1025–1048.
75 K. Takata, R. Osaka, Y. Matsushita and T. Nakanishi, *Surf Interface Anal*, 2020, **52**, 1029–1033.
76 T. Li, X. Bai, U. Gulzar, Y.-J. Bai, C. Capiglia, W. Deng, X. Zhou, Z. Liu, Z. Feng and R. Proietti Zaccaria, 2019, **29**, 1901730.
77 W.-P. Wang, J. Zhang, J. Chou, Y.-X. Yin, Y. You, S. Xin and Y.-G. Guo, *Advanced Energy Materials*, 2020, **11**, 2000791.
78 J. Zagórski, B. Silván, D. Saurel, F. Aguesse and A. Llordés, *ACS Appl. Energy Mater.*, 2020, **3**, 8344–8355.
79 D. Cheng, T. A. Wynn, X. Wang, S. Wang, M. Zhang, R. Shimizu, S. Bai, H. Nguyen, C. Fang, M. Kim, W. Li, B. Lu, S. J. Kim and Y. S. Meng, *Joule*, 2020, **4**, 2484–2500.
80 X. Li, Z. Ren, M. Norouzi Banis, S. Deng, Y. Zhao, Q. Sun, C. Wang, X. Yang, W. Li, J. Liang, X. Li, Y. Sun, K. Adair, R. Li, Y. Hu, T.-K. Sham, H. Huang, L. Zhang, S. Lu, J. Luo and X. Sun, *ACS Energy Letters*, 2019, **4**, 2480–2488.
81 I. Utke, S. Moshkalev and P. Russell, Eds., *Nanofabrication using focused ion and electron beams: principles and applications*, Oxford University Press, Oxford ; New York, 2012.
82 T. Shi, Y.-Q. Zhang, Q. Tu, Y. Wang, M. C. Scott and G. Ceder, *J. Mater. Chem. A*, 2020, **8**, 17399–17404.
83 F. Zhang, Q.-A. Huang, Z. Tang, A. Li, Q. Shao, L. Zhang, X. Li and J. Zhang, *Nano Energy*, 2020, **70**, 104545.
84 R. Ruess, S. Schweidler, H. Hemmelmann, G. Conforto, A. Bielefeld, D. A. Weber, J. Sann, M. T. Elm and J. Janek, *J. Electrochem. Soc.*, 2020, **167**, 100532.
85 R. Koerver, W. Zhang, L. de Biasi, S. Schweidler, A. O. Kondrakov, S. Kolling, T. Brezesinski, P. Hartmann, W. G. Zeier and J. Janek, *Energy Environ. Sci*, 2018, **11**, 2142–2158.
86 S. Choi, M. Jeon, J. Ahn, W. D. Jung, S. M. Choi, J.-S. Kim, J. Lim, Y.-J. Jang, H.-G. Jung, J.-H. Lee, B.-I. Sang and H. Kim, *ACS Appl. Mater. Interfaces*, 2018, **10**, 23740–23747.
87 V. Vanpeene, J. Villanova, J.-P. Suuronen, A. King, A. Bonnin, J. Adrien, E. Maire and L. Roué, *Nano Energy*, 2020, **74**, 104848.
88 P. Baudry, M. Armand, M. Gauthier and J. Masounave, *Solid State Ionics*, 1988, **28–30**, 1567–1571.
89 K. Zaghib, *J. Electrochem. Soc.*, 1998, **145**, 3135.
90 P. Hovington, M. Lagacé, A. Guerfi, P. Bouchard, A. Mauger, C. M. Julien, M. Armand and K. Zaghib, *Nano Lett.*, 2015, **15**, 2671–2678.
91 M. Golozar, P. Hovington, A. Paolella, S. Bessette, M. Lagacé, P. Bouchard, H. Demers, R. Gauvin and K. Zaghib, *Nano Lett.*, 2018, **18**, 7583–7589.
92 A. Brazier, L. Dupont, L. Dantras-Laffont, N. Kuwata, J. Kawamura and J. M. Tarascon, *Chem. Mater.*, 2008, **20**, 2352–2359.
93 K. Yamamoto, R. Yoshida, T. Sato, H. Matsumoto, H. Kurobe, T. Hamanaka, T. Kato, Y. Iriyama and T. Hirayama, *J. Power Sources*, 2014, **266**, 414–421.
94 D. Santhanagopalan, D. Qian, T. McGilvray, Z. Wang, F. Wang, F. Camino, J. Graetz, N. Dudney and Y. S. Meng, *The Journal of Physical Chemistry Letters*, 2014, **5**, 298–303.

95 Y. Cheng, L. Zhang, Q. Zhang, J. Li, Y. Tang, C. Delmas, T. Zhu, M. Winter, M.-S. Wang and J. Huang, *Materials Today*, 2020, **42**, 137–161.
96 Y. Wu and N. Liu, *Chem*, 2018, **4**, 438–465.
97 Z. Wang, D. Santhanagopalan, W. Zhang, F. Wang, H. L. Xin, K. He, J. Li, N. Dudney and Y. S. Meng, *Nano Lett.*, 2016, **16**, 3760–3767.
98 Y. Gong, J. Zhang, L. Jiang, J.-A. Shi, Q. Zhang, Z. Yang, D. Zou, J. Wang, X. Yu, R. Xiao, Y.-S. Hu, L. Gu, H. Li and L. Chen, *J. Am. Chem. Soc.*, 2017, **139**, 4274–4277.
99 Y. Gong, Y. Chen, Q. Zhang, F. Meng, J. A. Shi, X. Liu, X. Liu, J. Zhang, H. Wang, J. Wang, Q. Yu, Z. Zhang, Q. Xu, R. Xiao, Y. S. Hu, L. Gu, H. Li, X. Huang and L. Chen, *Nat Commun*, 2018, **9**, 3341.
100 Y. Nomura, K. Yamamoto, T. Hirayama, M. Ohkawa, E. Igaki, N. Hojo and K. Saitoh, *Nano Lett.*, 2018, **18**, 5892–5898.
101 Y. Nomura, K. Yamamoto, M. Fujii, T. Hirayama, E. Igaki and K. Saitoh, *Nature Communications*, 2020, **11**, 2824.
102 K. Yamamoto, Y. Iriyama, T. Asaka, T. Hirayama, H. Fujita, C. A. J. Fisher, K. Nonaka, Y. Sugita and Z. Ogumi, *Angew. Chem. Int. Ed.*, 2010, **49**, 4414–4417.
103 L. Wang, R. Xie, B. Chen, X. Yu, J. Ma, C. Li, Z. Hu, X. Sun, C. Xu, S. Dong, T.-S. Chan, J. Luo, G. Cui and L. Chen, *Nat Commun*, 2020, **11**, 5889.
104 N. J. J. de Klerk and M. Wagemaker, *ACS Applied Energy Materials*, 2018, **1**, 5609–5618.
105 S. P. Culver, R. Koerver, W. G. Zeier and J. Janek, *Advanced Energy Materials*, 2019, **9**, 1900626.
106 Y. Nomura, K. Yamamoto, T. Hirayama, S. Ouchi, E. Igaki and K. Saitoh, *Angew. Chem. Int. Ed.*, 2019, **58**, 5292–5296.
107 M. Weiss, F. J. Simon, M. R. Busche, T. Nakamura, D. Schröder, F. H. Richter and J. Janek, *Electrochem. Energ. Rev.*, 2020, **3**, 221–238.
108 J. Conder, C. Marino, P. Novák and C. Villevieille, *Journal of Materials Chemistry A*, 2018, **6**, 3304–3327.
109 J. Wolstenholme, *Auger electron spectroscopy: practical application to materials analysis and characterization of surfaces, interfaces, and thin films*, Momentum Press, 2015.
110 S. Hofmann, *Auger- and X-Ray Photoelectron Spectroscopy in Materials Science*, Springer Berlin Heidelberg, Berlin, Heidelberg, 2013, vol. 49.
111 S. Ichimura, H. E. Bauer, H. Seiler and S. Hofmann, *Surf. Interface Anal.*, 1989, **14**, 250–256.
112 J. Kikuma, T. Konishi and T. Sekine, *Journal of Electron Spectroscopy and Related Phenomena*, 1994, **69**, 141–147.
113 Y. Zhou, C. Doerrer, J. Kasemchainan, P. G. Bruce, M. Pasta and L. J. Hardwick, *Batteries & Supercaps*, 2020, **3**, 647–652.
114 B. Sun, C. Xu, J. Mindemark, T. Gustafsson, K. Edström and D. Brandell, *Journal of Materials Chemistry A*, 2015, **3**, 13994–14000.
115 J. Liang, D. Chen, K. Adair, Q. Sun, N. G. Holmes, Y. Zhao, Y. Sun, J. Luo, R. Li, L. Zhang, S. Zhao, S. Lu, H. Huang, X. Zhang, C. V. Singh and X. Sun, *Adv. Energy Mater.*, 2020, **11**, 2002455.
116 S. A. Pervez, B. P. Vinayan, M. A. Cambaz, G. Melinte, T. Diemant, T. Braun, G. Karkera, R. J. Behm and M. Fichtner, *J. Mater. Chem. A*, 2020, **8**, 16451–16462.
117 J. Qiu, X. Liu, R. Chen, Q. Li, Y. Wang, P. Chen, L. Gan, S.-J. Lee, D. Nordlund, Y. Liu, X. Yu, X. Bai, H. Li and L. Chen, *Adv. Funct. Mater.*, 2020, **30**, 1909392.
118 O. Sheng, J. Zheng, Z. Ju, C. Jin, Y. Wang, M. Chen, J. Nai, T. Liu, W. Zhang, Y. Liu and X. Tao, *Adv. Mater.*, 2020, **32**, 2000223.
119 S. Wenzel, T. Leichtweiss, D. Krüger, J. Sann and J. Janek, *Solid State Ionics*, 2015, **278**, 98–105.
120 Z. Liu, A. Borodin, G. Li, X. Liu, Y. Li and F. Endres, *J. Phys. Chem. C*, 2019, **124**, 300–308.
121 J. G. Connell, T. Fuchs, H. Hartmann, T. Krauskopf, Y. Zhu, J. Sann, R. Garcia-Mendez, J. Sakamoto, S. Tepavcevic and J. Janek, *Chem. Mater.*, 2020, **32**, 10207–10215.
122 N. Wu, P.-H. Chien, Y. Li, A. Dolocan, H. Xu, B. Xu, N. S. Grundish, H. Jin, Y.-Y. Hu and J. B. Goodenough, *J. Am. Chem. Soc.*, 2020, **142**, 2497–2505.
123 Y. Yamagishi, H. Morita, Y. Nomura and E. Igaki, *ACS Appl. Mater. Interfaces*, 2020, **13**, 580–586.
124 R. Koerver, F. Walther, I. Aygün, J. Sann, C. Dietrich, W. G. Zeier and J. Janek, *Journal of Materials Chemistry A*, 2017, **5**, 22750–22760.
125 S.-M. Bak, Z. Shadike, R. Lin, X. Yu and X.-Q. Yang, *NPG Asia Materials*, 2018, **10**, 563–580.
126 M. Mirolo, D. Leanza, L. Höltschi, C. Jordy, V. Pelé, P. Novák, M. El Kazzi and C. A. F. Vaz, *Anal. Chem.*, 2020, **92**, 3023–3031.
127 Z. Wang, M. Kotobuki, L. Lu and K. Zeng, *Electrochimica Acta*, 2020, **334**, 135553.
128 P. Vadhva, J. Hu, M. J. Johnson, R. Stocker, M. Braglia, D. J. L. Brett and A. J. E. Rettie, *ChemElectroChem*, , DOI:10.1002/celc.202100108.

129 J. F. M. Oudenhoven, F. Labohm, M. Mulder, R. A. H. Niessen, F. M. Mulder and P. H. L. Notten, *Adv. Mater. (Weinheim, Ger.)*, 2011, **23**, 4103–4106.

130 C. Wang, Y. Gong, J. Dai, L. Zhang, H. Xie, G. Pastel, B. Liu, E. Wachsman, H. Wang and L. Hu, *J. Am. Chem. Soc.*, 2017, **139**, 14257–14264.

131 F. Han, A. S. Westover, J. Yue, X. Fan, F. Wang, M. Chi, D. N. Leonard, N. J. Dudney, H. Wang and C. Wang, *Nature Energy*, 2019, **4**, 187–196.

132 Q. Li, T. Yi, X. Wang, H. Pan, B. Quan, T. Liang, X. Guo, X. Yu, H. Wang, X. Huang, L. Chen and H. Li, *Nano Energy*, 2019, **63**, 103895.

133 W. Ping, C. Wang, Z. Lin, E. Hitz, C. Yang, H. Wang and L. Hu, *Advanced Energy Materials*, 2020, **10**, 2000702.

134 L. R. Mangani and C. Villevieille, *J. Mater. Chem. A*, 2020, **8**, 10150–10167.

135 W. Zhang, D. Schröder, T. Arlt, I. Manke, R. Koerver, R. Pinedo, D. A. Weber, J. Sann, W. G. Zeier and J. Janek, *Journal of Materials Chemistry A*, 2017, **5**, 9929–9936.

136 K. J. Harry, D. T. Hallinan, D. Y. Parkinson, A. A. MacDowell and N. P. Balsara, *Nat. Mater.*, 2014, **13**, 69–73.

137 J. A. Maslyn, W. S. Loo, K. D. McEntush, H. J. Oh, K. J. Harry, D. Y. Parkinson and N. P. Balsara, *J. Phys. Chem. C*, 2018, **122**, 26797–26804.

138 L. Frenck, J. A. Maslyn, W. S. Loo, D. Y. Parkinson and N. P. Balsara, *ACS Appl. Mater. Interfaces*, 2019, **11**, 47878–47885.

139 J. A. Maslyn, L. Frenck, W. S. Loo, D. Y. Parkinson and N. P. Balsara, *ACS Applied Energy Materials*, 2019, **2**, 8197–8206.

140 A. S. Ho, P. Barai, J. A. Maslyn, L. Frenck, W. S. Loo, D. Y. Parkinson, V. Srinivasan and N. P. Balsara, *ACS Appl. Energy Mater.*, 2020, **3**, 9645–9655.

141 J. Tippens, J. C. Miers, A. Afshar, J. A. Lewis, F. J. Q. Cortes, H. Qiao, T. S. Marchese, C. V. Di Leo, C. Saldana and M. T. McDowell, *ACS Energy Letters*, 2019, **4**, 1475–1483.

142 N. Sun, Q. Liu, Y. Cao, S. Lou, M. Ge, X. Xiao, W.-K. Lee, Y. Gao, G. Yin, J. Wang and X. Sun, *Angew. Chem. Int. Ed.*, 2019, **58**, 18647–18653.

143 X. Wu, J. Billaud, I. Jerjen, F. Marone, Y. Ishihara, M. Adachi, Y. Adachi, C. Villevieille and Y. Kato, *Advanced Energy Materials*, 2019, **9**, 1901547.

144 Y. Kimura, A. Tomura, M. Fakkao, T. Nakamura, N. Ishiguro, O. Sekizawa, K. Nitta, T. Uruga, T. Okumura, M. Tada, Y. Uchimoto and K. Amezawa, *The Journal of Physical Chemistry Letters*, 2020, **11**, 3629–3636.

145 Y. Kimura, M. Fakkao, T. Nakamura, T. Okumura, N. Ishiguro, O. Sekizawa, K. Nitta, T. Uruga, M. Tada, Y. Uchimoto and K. Amezawa, *ACS Appl. Energy Mater.*, 2020, **3**, 7782–7793.

146 J.-P. Barnes, L. Djomeni, S. Minoret, T. Mourier, J.-M. Fabbri, G. Audoit and S. Fadloun, *Journal of Vacuum Science & Technology B, Nanotechnology and Microelectronics: Materials, Processing, Measurement, and Phenomena*, 2016, **34**, 03H137.

147 A. Priebe, P. Bleuet, G. Goret, J. Laurencin, D. Montinaro and J.-P. Barnes, *Microsc Microanal*, 2016, **22**, 1261–1269.

148 T. Zou and P. J. Sadler, *Drug Discovery Today: Technologies*, 2015, **16**, 7–15.

149 B. Reif, S. E. Ashbrook, L. Emsley and M. Hong, *Nat Rev Methods Primers*, 2021, **1**, 2.

150 S. E. Ashbrook and P. Hodgkinson, *The Journal of Chemical Physics*, 2018, **149**, 040901.

151 X. Liu, Z. Liang, Y. Xiang, M. Lin, Q. Li, Z. Liu, G. Zhong, R. Fu and Y. Yang, *Adv. Mater.*, 2021, 2005878.

152 C. Yu, S. Ganapathy, N. J. J. de Klerk, I. Roslon, E. R. H. van Eck, A. P. M. Kentgens and M. Wagemaker, *J. Am. Chem. Soc.*, 2016, **138**, 11192–11201.

153 C. Yu, S. Ganapathy, E. R. H. van Eck, H. Wang, S. Basak, Z. Li and M. Wagemaker, *Nat Commun*, 2017, **8**, 1086.

154 Z. Cheng, M. Liu, S. Ganapathy, C. Li, Z. Li, X. Zhang, P. He, H. Zhou and M. Wagemaker, *Joule*, 2020, **4**, 1311–1323.

155 S. Ganapathy, C. Yu, E. R. H. van Eck and M. Wagemaker, *ACS Energy Lett.*, 2019, **4**, 1092–1097.

156 J. Zagórski, J. M. López del Amo, M. J. Cordill, F. Aguesse, L. Buannic and A. Llordés, *ACS Applied Energy Materials*, 2019, **2**, 1734–1746.

157 C.-Z. Zhao, X.-Q. Zhang, X.-B. Cheng, R. Zhang, R. Xu, P.-Y. Chen, H.-J. Peng, J.-Q. Huang and Q. Zhang, *Proc Natl Acad Sci USA*, 2017, **114**, 11069–11074.

158 S. H.-S. Cheng, K.-Q. He, Y. Liu, J.-W. Zha, M. Kamruzzaman, R. L.-W. Ma, Z.-M. Dang, R. K. Y. Li and C. Y. Chung, *Electrochimica Acta*, 2017, **253**, 430–438.

159 P. Ranque, J. Zagórski, S. Devaraj, F. Aguesse and J. M. López del Amo, *J. Mater. Chem. A*, 2021, **9**, 17812–17820.

160 L. E. Marbella, S. Zekoll, J. Kasemchainan, S. P. Emge, P. G. Bruce and C. P. Grey, *Chem. Mater.*, 2019, **31**, 2762–2769.

161 B. Tsuchiya, J. Ohnishi, Y. Sasaki, T. Yamamoto, Y. Yamamoto, M. Motoyama, Y. Iriyama and K. Morita, *Advanced Materials Interfaces*, 2019, **6**, 1900100.

162 Y. Liu, Q. Sun, J. Liu, M. Norouzi Banis, Y. Zhao, B. Wang, K. Adair, Y. Hu, Q. Xiao, C. Zhang, L. Zhang, S. Lu, H. Huang, X. Song and X. Sun, *ACS Appl. Mater. Interfaces*, 2020, **12**, 2293–2298.

163 H. Kiuchi, K. Hikima, K. Shimizu, R. Kanno, F. Toshiharu and E. Matsubara, *Electrochemistry Communications*, 2020, **118**, 106790.

164 A. Regoutz, M. Mascheck, T. Wiell, S. K. Eriksson, C. Liljenberg, K. Tetzner, B. A. D. Williamson, D. O. Scanlon and P. Palmgren, *Review of Scientific Instruments*, 2018, **89**, 073105.

165 L.-P. Hou, X.-Q. Zhang, B.-Q. Li and Q. Zhang, *Angew. Chem. Int. Ed.*, 2020, **59**, 15109–15113.

166 K. N. Wood and G. Teeter, *ACS Applied Energy Materials*, 2018, **1**, 4493–4504.

167 S.-K. Otto, Y. Moryson, T. Krauskopf, K. Peppler, J. Sann, J. Janek and A. Henss, *Chem. Mater.*, 2021, **33**, 859–867.

168 C. M. Mahoney, *Mass Spectrom. Rev.*, 2010, **29**, 247–293.

169 K. Ridier, D. Aureau, B. Bérini, Y. Dumont, N. Keller, J. Vigneron, A. Etcheberry and A. Fouchet, *J. Phys. Chem. C*, 2016, **120**, 21358–21363.

170 F. J. Simon, M. Hanauer, A. Henss, F. H. Richter and J. Janek, *ACS Appl. Mater. Interfaces*, 2019, **11**, 42186–42196.

171 L. Somerville, J. Bareño, P. Jennings, A. McGordon, C. Lyness and I. Bloom, *Electrochimica Acta*, 2016, **206**, 70–76.

172 C.-Y. Tang, R. T. Haasch and S. J. Dillon, *Chem. Commun. (Cambridge, U. K.)*, 2016, **52**, 13257–13260.

173 C.-Y. Tang, K. Leung, R. T. Haasch and S. J. Dillon, *ACS Appl. Mater. Interfaces*, 2017, **9**, 33968–33978.

174 C.-Y. Tang, L. Feng, R. T. Haasch and S. J. Dillon, *Electrochim. Acta*, 2018, **277**, 197–204.

175 A. U. Chowdhury, N. Muralidharan, C. Daniel, R. Amin and I. Belharouak, *Journal of Power Sources*, 2021, **506**, 230173.

176 N. G. Rey and D. D. Dlott, *J. Electroanal. Chem.*, 2017, **800**, 114–125.

177 S. A. Shah and S. Baldelli, *Acc. Chem. Res.*, , DOI:10.1021/acs.accounts.0c00057.

178 A. M. Gardner, K. H. Saeed and A. J. Cowan, *Phys. Chem. Chem. Phys.*, 2019, **21**, 12067–12086.

179 Y. Horowitz, H.-L. Han, F. A. Soto, W. T. Ralston, P. B. Balbuena and G. A. Somorjai, *Nano Lett.*, 2018, **18**, 1145–1151.

180 H. Liu, Y. Tong, N. Kuwata, M. Osawa, J. Kawamura and S. Ye, *J. Phys. Chem. C*, 2009, **113**, 20531–20534.

181 L. Yu, H. Liu, Y. Wang, N. Kuwata, M. Osawa, J. Kawamura and S. Ye, *Angew. Chem. Int. Ed.*, 2013, **52**, 5753–5756.

182 J. Dawidowski, J. R. Granada, J. R. Santisteban, F. Cantargi and L. A. R. Palomino, in *Experimental Methods in the Physical Sciences*, Elsevier, 2013, vol. 44, pp. 471–528.

183 L. Hoeltshi, M. Cochet, P. Trtik, C. Jordy, C. Villevieille and P. Boillat, in *ECS Meeting Abstracts*, The Electrochemical Society, 2019.